ornl

NUREG/CR-3599
ORNL/Sub/82-22252/2

OAK RIDGE
NATIONAL
LABORATORY

MARTIN MARIETTA

Sources of Uncertainty in the Calculation of Loads on Supports of Piping Systems

E. C. Rodabaugh

Work Performed for
U.S. Nuclear Regulatory Commission
Office of Nuclear Regulatory Research
Under Interagency Agreement DOE 40-550-75
NRC FIN No. B0474

OPERATED BY
MARTIN MARIETTA ENERGY SYSTEMS, INC.
FOR THE UNITED STATES
DEPARTMENT OF ENERGY

Printed in the United States of America. Available from
National Technical Information Service
U.S. Department of Commerce
5285 Port Royal Road, Springfield, Virginia 22161

Available from

GPO Sales Program
Division of Technical Information and Document Control
U.S. Nuclear Regulatory Commission
Washington, D.C. 20555

NUREG/CR-3599
ORNL/Sub/82-22252/2
Dist. Category RM

Engineering Technology Division

SOURCES OF UNCERTAINTY IN THE CALCULATION OF LOADS ON SUPPORTS OF PIPING SYSTEMS

E. C. Rodabaugh

Manuscript Completed — May 1, 1984
Date Published — June 1984

Report Prepared by
E. C. Rodabaugh Associates, Inc.
4625 Cemetery Road
Hilliard, Ohio 43026
under
Subcontract No. 19X-22252C

Work Performed for
U.S. Nuclear Regulatory Commission
Office of Nuclear Regulatory Research
under
DOE Interagency Agreement No. 40-550-75

NRC FIN No. B0474

OAK RIDGE NATIONAL LABORATORY
Oak Ridge, Tennessee 37831
operated by
MARTIN MARIETTA ENERGY SYSTEMS, INC.
for the
U.S. DEPARTMENT OF ENERGY
under Contract No. DE-AC05-840R21400

CONTENTS

FOREWORD

The work reported here was sponsored by the U.S. Nuclear Regulatory Commission's (NRC) ASME Code Section III — Technical Support Program, which is managed at ORNL by G. T. Yahr. It was performed under a subcontract to E. C. Rodabaugh Associates that was monitored by S. E. Moore. The original manager for the NRC, E. T. Baker, was succeeded by D. J. Guzy.

NOMENCLATURE

a_n	$[mw_n^2/(EI)]^{1/4}$
C_2	stress index for elbows = $1.95/h^{2/3}$
D	mean diameter of vessel or run pipe (Fig. 6)
d	mean diameter of branch pipe (Fig. 6)
E	modulus of elasticity
F_x	support force [Fig. 4(*a*)]
F_y	support force [Fig. 4(*a*)]
F_{1x}	support force [Fig. 4(*c*)]
F_{2x}	support force [Fig. 4(*c*)]
F_{1y}	support force [Fig. 4(*c*)]
F_{2y}	support force [Fig. 4(*c*)]
$f(\lambda)$	$= M/ET^3\phi^0$ (from Ref. 11)
h	elbow parameter = tR/r^2
i	stress intensification factor for elbows = $0.9/h^{2/3}$
I	moment of inertia of pipe cross section
I_b	moment of inertia of branch pipe = $\pi d^3 t/8$
k	flexibility factor
k_b	nozzle flexibility factor
k_{x3}	nozzle flexibility factor for M_{x3} (Fig. 6)
k_{y3}	nozzle flexibility factor for M_{y3} (Fig. 6)
k_{z3}	nozzle flexibility factor for M_{z3} (Fig. 6)
k_{ep}	plastic-elbow flexibility factor
L_1	leg length (Fig. 4)
L_2	leg length (Fig. 4)
m	mass per unit length
M	moment
M_1	support moment (Fig. 4)
M_2	support moment (Fig. 4)
M_e	elbow moment [Fig. 4(*a*)]
M_j	corner moment [Fig. 4(*c*)]
M_i	in-plane elbow moment (Fig. 3)
M_o	out-of-plane elbow moment (Fig. 3)
M_t	torsional elbow moment (Fig. 3)

P	internal pressure
Q	dynamic-load parameter [Eq. (A.39)]
$[q(x)]_f$	dynamic-load parameter [Eq. (A.38)]
R	bend radius of elbow (Fig. 3)
r	cross section radius of elbow (Fig. 3)
S	allowable stress, Code[1] Class 2 or 3 component
S_c	allowable stress at cold end of cycle, Code[1] Class 2 or 3 component
S_h	allowable stress at hot end of cycle, Code[1] Class 2 or 3 component
S_m	allowable stress intensity, Code[1] Class 1 component
S_y	material yield strength
T	wall thickness of vessel or run pipe
T	temperature (Sect. 8)
t	wall thickness of elbow (Sect. 3)
t	wall thickness of branch pipe (Sect. 4)
t_n	wall thickness of nozzle (Fig. 6)
W	concentrated weight [Fig. 4(*b*)]
w_n	natural frequency of nth mode
Z	section modulus of pipe cross section
α	elbow arc angle (Sect. 3), also coefficient of thermal expansion
γ	Elbow parameter = $(\pi/2)(a_n L_1)(R/L_1)k$ [Eq. (9)]
γ_b	Nozzle parameter = $(a_n L_1)k_b d/L_1$ [Eq. (16)]
ΔT	change in average temperature of a piping system
θ	rotation of one end of an elbow with respect to the other end
λ	$(d/D)\sqrt{D/T}$
Λ	$(L/D)\sqrt{D/T}$, L = length of vessel between supports
ϕ	rotation of nozzle with respect to vessel or run pipe surface

SOURCES OF UNCERTAINTY IN THE CALCULATION OF LOADS ON SUPPORTS OF PIPING SYSTEMS

E. C. Rodabaugh

ABSTRACT

Loads on piping supports are obtained from an analysis of the piping system. The analysis involves uncertainties from various sources. These sources of uncertainties are discussed and ranges of uncertainties are illustrated by simple examples. The sources of uncertainty are summarized and assigned a judgmental ranking of the typical relative significance of the uncertainty.

---

1. INTRODUCTION

Failure of one or more supports* of a piping system does not necessarily lead to a leak or break in the piping pressure boundary. However, failure of supports may lead to large displacements which, in extreme cases, could permit the pipe to strike adjacent equipment or reduce the flow capacity of the pipe. Failures of supports could also lead to higher-than-anticipated loads on pumps, compressors, heat exchangers, valves, or other equipment attached to the piping.

Failure of a support, depending upon its function, may not be significant until a rupture occurs (e.g., fracture of a hanger rod or pull out of bolts holding the support to a concrete structure). However, gross plastic deformation of the support may be considered to be a failure in that it may permit unanticipated large displacements and loads on attached equipment.

The objective of this report is to describe and discuss the sources of uncertainty in the calculation of piping support loads as obtained from an analysis of the piping system. Sections 2 through 7 deal with elastic (but not necessarily linear) responses of the piping and supports to static or dynamic applied loads. Section 2 is a brief overview of how piping system analyses are performed and some of the uncertainties involved in this process. Section 3 discusses elbow flexibility and, using some simple examples, indicates how elbow flexibility may change calculated support loads for both static and dynamic applied loads. Section 4 discusses nozzle flexibilities and presents available data, which can be used as a guide to estimate nozzle flexibility. These nozzle flexibilities are then used in some simple examples to indicate how they may change calculated support loads for both static and dynamic applied loads.

---

*The term "support" is used in this report to include such devices as hangers, spring or constant load hangers, guides, stops, and snubbers.

Sections 5, 6, and 7 describe, in conceptual terms, how the support characteristics (e.g., gaps), construction misalignment, and building structure rigidity might change calculated support loads. Section 8 discusses and gives some simple examples of the effects of inelastic behavior of the piping and discusses the effects of inelastic behavior of the supports in conceptual terms. Section 9 contains a discussion and summary, listing the many sources of uncertainties in calculating piping support loads.

Design or construction errors are also a source of uncertainties in calculated piping support loads, but this report does not address such errors.

Support loads for small-size (e.g., 2 NPS or smaller) piping systems are often estimated by so-called "chart methods." The uncertainties involved in such estimates are not addressed in this report.

2. PIPING SYSTEM MODELS

2.1 Piping Systems and Piping System Loads

Loads on piping supports are calculated by a piping system analysis. A piping system consists of the piping components (straight pipe, curved pipe, tees, valves, etc.) and the piping supports between two or more anchors. The piping system analytical model represents this complex assemblage of components and supports by straight- or curved-line segments as illustrated by Fig. 1. Except where a flexibility factor is used, the

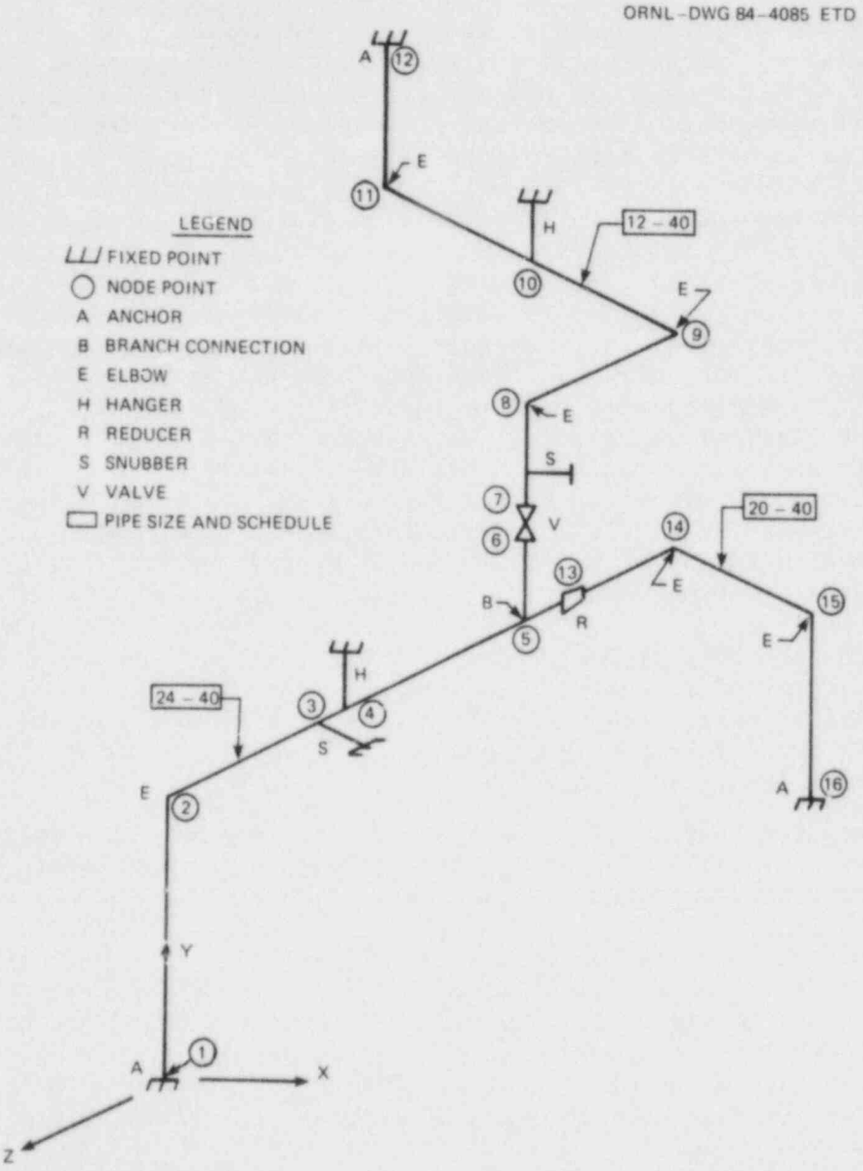

Fig. 1. Isometric of simple piping system.

resistance of these line segments to deformation is taken to be the same as straight pipe.

Loads on piping systems consist of

1. weight of piping components and their contained fluid and insulation;
2. restraint of thermal expansion;
3. dynamic effects such as water hammer, relief valve thrust, and earthquakes; and
4. wind and weight of ice or snow for outdoor piping.

2.2 Piping Dimensions and Properties

The overall dimensions of the piping system are described by global coordinates of "node points" (e.g., in Fig. 1, Node 3 is located at X = 0, Y = 8, Z = −4.5) in appropriate-length units. The pipe cross sections are assumed to have nominal dimensions (e.g., 12-in. NPS Schedule 40 pipe is assumed to have an outside diameter of 12.75 in. and a wall thickness of 0.406 in.). The stiffness is proportional to EI, where E is a Code* tabulated (Ref. 1) modulus of elasticity and I is the nominal moment of inertia of the pipe cross section (e.g., I = 300 in.^{4} for 12-in. Schedule 40 pipe).

Aside from design errors (e.g., node point has wrong coordinates) or construction errors (e.g., Schedule 80 pipe used rather than the Schedule 40 assumed in the analysis), these data are relatively accurate (±10%).

The flexibility of elbows is included in the model by use of Code-specified flexibility factors. As discussed in Sect. 3, significant uncertainty may arise from inaccurate elbow flexibility factors.

Nozzles are often considered to be anchors. As discussed in Sect. 4, nozzles may permit significant rotations; hence, the "anchor" assumption may introduce large uncertainties in calculated support loads.

Restraints may consist of

1. spring or constant-load hangers used for weight support;
2. relatively rigid members, such as tie rods; and
3. snubbers, which have negligible resistance to slow movement but act as rigid restraints for fast movement. These are used for restraint of dynamic loads (see Sect. 5.4).

Restraints may restrict displacement in one, two, or three directions. Guides may be used to restrict rotations as well as displacements. Stops permit a prescribed movement beyond which the stop prevents further movement.

These various restraints are usually included in the analytical model in an idealized manner (e.g., a tie rod prevents any displacement in the direction of the tie rod). The effect of the flexibility of the tie rod, local flexibility of the pipe (e.g., the pipe clamp), and any clearances that may exist are usually ignored. The effect of these flexibilities and clearances are discussed in Sect. 5. Further, the flexibility of supports

*The term "Code" in this report refers to the ASME Boiler and Pressure Vessel Code, Sect. III, Division 1 (see Ref. 1).

may depend upon the way they are attached to the building and the flexibility of the building. This is discussed in Sect. 7.

2.3 Input Load Description

2.3.1 Weight and restraint of thermal expansion

Weight of the pipe, fluid contents, and insulation are nominal weights but are relatively accurate. However, these distributed weights may be included in the analytical model as lumped masses. The number and spacing of the lumped masses is usually governed by the requirements for an adequate dynamic analysis; this usually ensures adequate representation of distributed weights for the static weight evaluation. Valves and valve operators are also represented by lumped masses. Usually two masses are used: one represents the valve mass, and the other, the valve operator mass, connected by a line element with stiffness representing that of the valve-to-operator connecting structure. Evaluation of the weight loads is deemed to be accurate within about ±20%. Large uncertainties may exist in the weights of ANSI B16.9 tees and elbows and in the flexibility of elbows. The effect on flexibility of over-nominal-thickness elbows is discussed in Sect. 3.2.

Unrestrained thermal expansion is calculated by the product $\alpha\Delta TL$, where α is the coefficient of thermal expansion, ΔT is the change in temperature, and L is the length in a given direction. To the extent that the piping system is connected to equipment that changes temperature, the thermal expansion of that equipment is included in the restraint of thermal expansion evaluation. Values of α and L are accurately known (±10%), and the value of ΔT is also accurately known for a relatively slow fluid temperature transient throughout the piping system. However, for rapid fluid temperature transients or where branch lines are subjected to different fluid flow conditions, the appropriate value(s) of ΔT (several different values of ΔT may be needed to represent the thermal expansion) may be uncertain. Several bounding calculations may be needed to represent changes in the system as a function of time.

Under some fluid-flow conditions, a thermal gradient may exist around the circumference of the pipe (e.g., the top of the pipe may be hotter than the bottom or vice versa). This type of thermal gradient produces bowing of an unrestrained pipe, which leads to the equivalent of additional "free thermal expansion" that is seldom considered in piping system analyses.

2.3.2 Dynamic loads

For earthquake evaluation, the input consists of motion of the piping system support points. Usually, this input is derived from floor response spectra in which acceleration is given as a function of frequency for specified amounts of damping (e.g., 2% of critical damping).

The piping-input response spectrum is usually an envelope of the response at all support points. The peaks are broadened by ±15% to partially compensate for inaccuracies in floor response spectra and in the

calculated piping system frequencies. This is an important aspect because, as illustrated in Fig. 2, the input acceleration varies rapidly with frequency and a small error in the calculated frequency could lead to a large theoretical error in the calculated support loads.

The floor response spectra are determined by an evaluation of the building response to the postulated earthquake. The characteristics and frequency of occurrence of earthquakes at a given site are subject to large uncertainties. For example, the operating basis earthquake (OBE) is typically expected to occur once in one hundred years, and the safe shutdown earthquake (SSE), once in one thousand years. However, because this is a probability estimate based on limited data, one cannot say with certainty that an earthquake larger than the SSE will not occur.

Additional uncertainties exist in the piping system evaluation in that an earthquake produces both horizontal and vertical ground motions. For a nonplanar piping system, "horizontal" is an infinity of directions, each of which would lead to a different piping system response. The usual procedure consists of calculating responses for two horizontal directions that are 90° apart and then combining the two responses with the vertical-motion response. The combination is usually done by $R = (R_{h1}^2 + R_{h2}^2 + R_v^2)^{1/2}$. This "square root of the sum of the squares" (SRSS) method has some probabilistic basis.

Earthquake evaluations obviously are subject to large uncertainties. However, the present day procedures for earthquake evaluation tend to be conservative because of the use of low damping factors and response-spectra analyses rather than time-history analyses and because inelastic effects are ignored. Accordingly, the evaluations tend to overestimate loads on the supports for the postulated OBE and SSE for a given nuclear power plant.

For water-hammer or relief-valve thrust, the load input data usually consist of a time-history of forcing functions. These forcing functions are derived from fluid-flow momentum change evaluations. An appropriate damping factor must be estimated as input for the analysis. The dynamic analysis is subject to many of the uncertainties of an earthquake analysis (e.g., calculated natural frequencies). The input forcing functions are usually deterministic in nature, and the use of a time-history, rather than a response-spectrum approach, tends to produce results having lower uncertainties than for earthquake evaluations. However, some types of water hammer are difficult to anticipate or evaluate (e.g., control valve instability, pump startup into a partially empty line, or steam bubble collapse). Large uncertainties exist for these types of water hammer, and the best defense usually consists of design features and operating procedures that minimize the occurrence and/or severity of such types of water hammer.

2.4 Elastic Analysis

Currently, routine piping system analyses are based on linear elastic piping system and support models. Nonlinear elastic effects are discussed in Sect. 3 (elbow, internal pressure) and Sect. 5 (gaps, nonlinearity of snubbers). A discussion of inelastic effects is presented in Sect. 8.

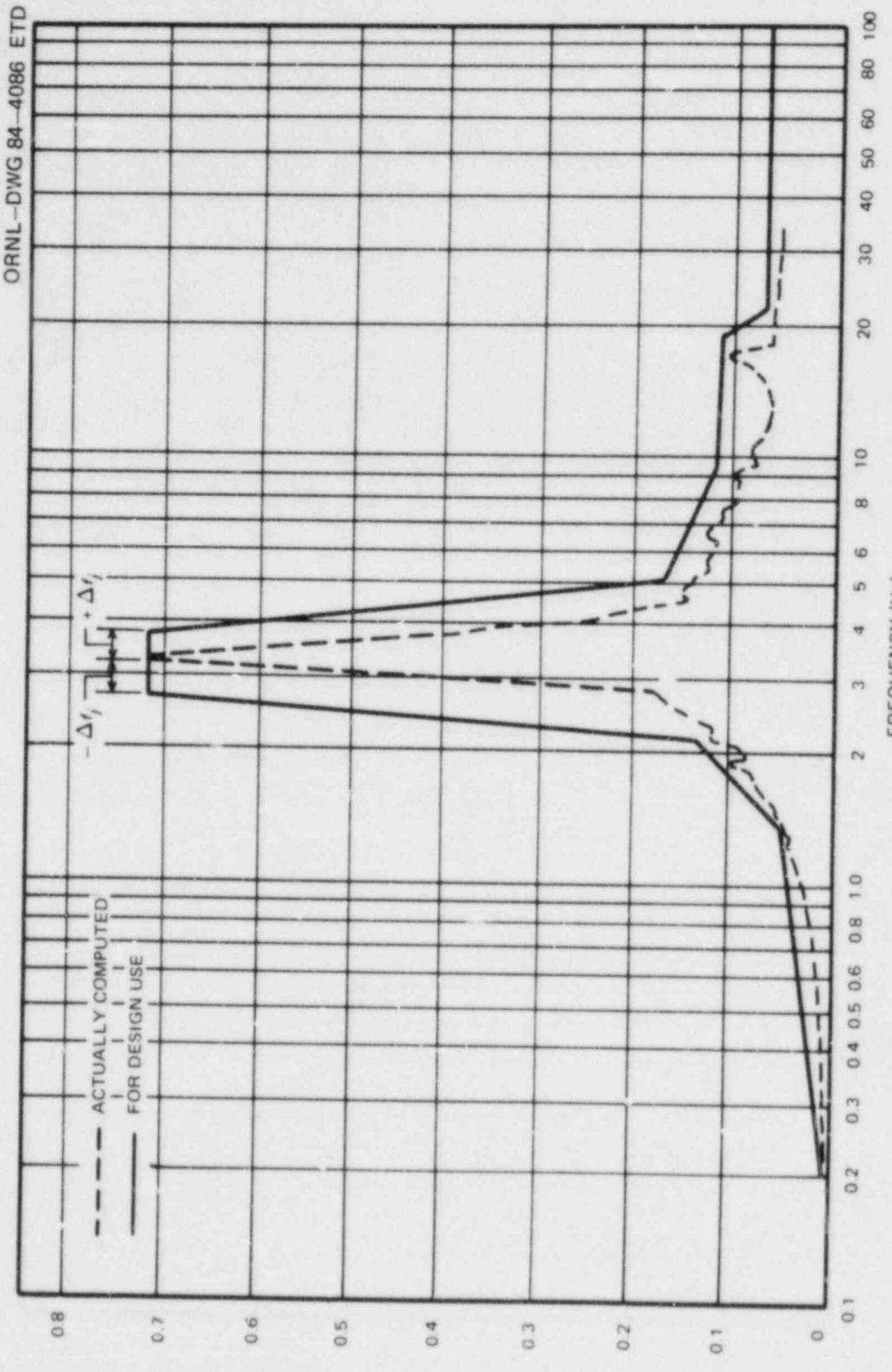

Fig. 2. Example of earthquake response spectrum (Fig. N-1226-1 of Code).

3. ELBOW FLEXIBILITY

3.1 No-End-Effects Theory

Flexibility factors for elbows (and curved pipe) that are routinely used in a piping system analysis are obtained by the equations

$$k = 1.65/h \geq 1.0 \quad \text{for } M_i \text{ and } M_o \,, \tag{1}$$

$$k = 1.00 \quad \text{for } M_t \,, \tag{2}$$

where $h = tR/r^2$ and M_i, M_o, and M_t are defined in Fig. 3.

Equations (1) and (2) are based on theories of a uniform-wall, toroidal shell and are included in the Code. The effect of whatever is attached to the ends of the elbow (e.g., straight pipe or pressure vessel nozzle) are ignored by the theory. Conditions under which Eqs. (1) and (2) may be inaccurate are discussed in the following.

Flexibility factors are used in piping system analyses in the form

$$\theta = \frac{kR}{EI} \int_o^\alpha M d\alpha \,. \tag{3}$$

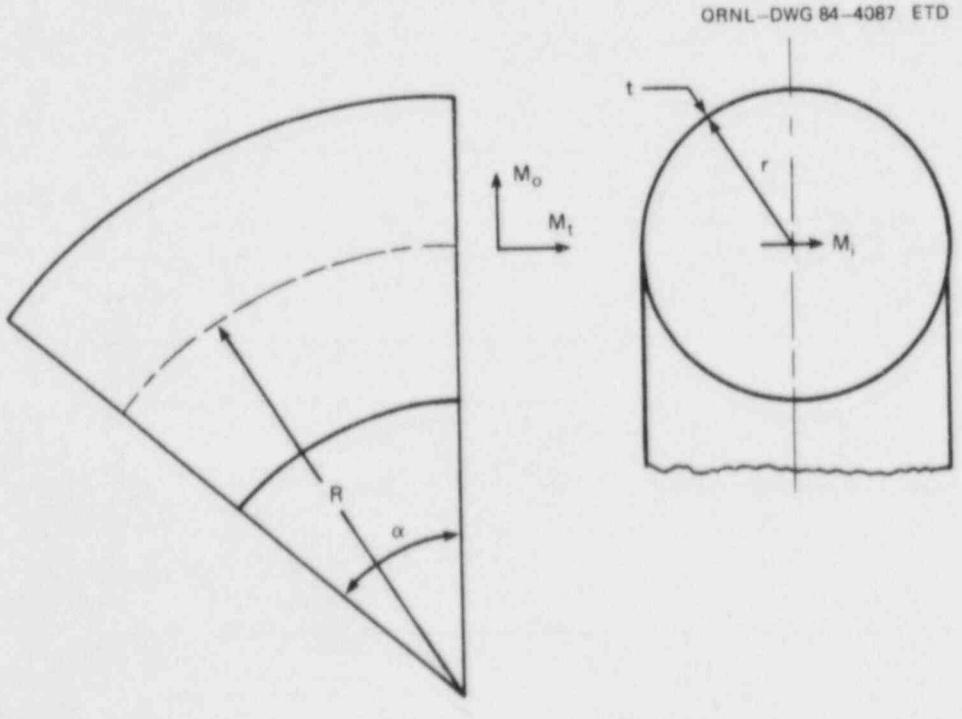

Fig. 3. Elbow nomenclature.

If, for example, M is constant through a 90° elbow, Eq. (3) gives

$$\theta = \frac{kRM}{EI}\frac{\pi}{2}, \qquad (4)$$

where θ is the rotation of one end of elbow with respect to the other end.

3.2 Nominal vs Actual Dimensions

Equation (1) is based on theories which assume that an elbow is a portion of a toroidal shell with t, r, and R constant. The effect of a smooth variation in thickness t around the cross section has been studied by Spence and Findlay;[2] their results indicate that a variation in t of ±20% produces about 5% variation in flexibility. Because thickness variations in typical elbows or bent pipe do not exceed ±20%, it appears that thickness variations are not significant in elbow flexibility.

The effect of variation in r (out-of-roundness) has been studied by Clark, Gilroy, and Reissner[3] and by Findlay and Spence.[4] The change in flexibility depends upon the orientation of the out-of-roundness with respect to the elbow. However, for any orientation, out-of-roundness (d_{max}/d_{min}, $d = 2r$) of up to 1.08 does not change the flexibility by more than about ±10%. Because out-of-roundness in typical elbows and bent pipe does not exceed 1.08, it appears that out-of-roundness effects have a minor effect on elbow flexibility.

Occasionally, an elbow may be purchased that has an average wall thickness that is significantly greater than nominal. This is because ANSI B16.9 (which includes elbows) does not contain a maximum thickness (or weight) limit. One could, for example, order a 30-in. by 0.375-in. wall elbow and receive a 30-in. elbow with 0.500-in. average wall taperbored at the ends to match a 0.375-in.-wall pipe. For that elbow, $k = 15.95$, rather than $k = 21.45$ for a 30-in.-wall elbow that might be used in the piping system analysis. Also, the moment of inertia would be higher by about 31%, so that the flexibility would be overestimated by a factor of $1.31 \times 21.45/15.95 = 1.76$. This could have a significant effect on calculated support loads.

3.3 Internal Pressure Effect

For Class 2 and 3 piping the Code does not consider the effect of internal pressure on elbow flexibility. For Class 1 piping, the Code gives the equation

$$k = (1.65/h)\,[1 + 6(Pr/tE)(r/t)^{4/3}\,(R/r)^{1/3}]^{-1} \geq 1.0\ . \qquad (5)$$

Equation (5) was developed by Rodabaugh and George[5] using "no-end-effects" theory. It is applicable to M_i and M_o as defined in Fig. 3. According to Eq. (5), k is a nonlinear function of internal pressure P.

To illustrate the significance of Eq. (5), we apply it to a 30-in. by 0.375-in. wall elbow having a 45-in. bend radius with pressure loading Pr/t = 15,000 psi. Pr/t is the nominal hoop stress resulting from internal pressure and 15,000 psi is the Code Class 2 or 3 allowable stress for SA-106 Grade B material at temperatures up to 650°F. Using $E = 2.79 \times 10^7$ psi, Eq. (5) gives

$$k = (1.65/h)\,[1 + 6(15{,}000)(39.5)^{4/3}\,(3.088)^{1/3}/(2.79 \times 10^7)]^{-1}$$

$$= (1.65/h)1.632\ . \qquad (6)$$

For the 30-in. elbow, $h = 0.375 \times 45/14.8125^2 = 0.0769$. Accordingly, $k = 13.15$ with an internal pressure corresponding to Pr/t = 15,000 psi (P = 1013 psi), compared with $k = 21.45$ when the internal pressure effect is ignored.

For most piping, r/t tends to be smaller than the 14.81 of the example and Pr/t tends to be less than the Code allowable stress. Hence, in most cases, the pressure effect is less than indicated by the example. Nevertheless, ignoring the internal pressure may lead to a significant overestimation of the elbow flexibility.

3.4 End Effects

The flexibility of an elbow derives from its tendency to become out-of-round when subjected to M_i or M_o loading. However, if ovalization is prevented by restraints at the ends of the elbow, for example, by a heavy clamp tightly secured to one end, Eq. (1) may overestimate the flexibility factor. Consequently, the piping system will be stiffer than calculated.

The subject of end-effects for straight pipe on elbows is discussed by Rodabaugh and Moore.[6] For in-plane moments on elbows in which $\alpha = 90°$, having straight pipe of at least two diameters in length attached to both ends, they found that the value of k is equal to 1.30/h (≥1.0) rather than 1.65/h (≥1.0) by Eq. (1).[6] For $\alpha = 45°$, $k = 1.1/h$ (≥1.0), and as $\alpha \to 0$, $k \to 1.0$ regardless of the value of h. Of course, for small α, the elbow flexibility does not contribute much to the piping sytem flexibility [see Eq. (3)].

For the considerably more complex out-of-plane moment (note that M_o on one end of a 90° elbow becomes a torsional moment M_t at the other end), Rodabaugh and Moore[6] suggests that $k = 1.25/h$ (≥1.0) for both M_o and M_i.

Although the straight-pipe end effects are not necessarily insignificant, if one or both ends of an elbow are restrained by something more rigid than straight pipe, the end effects become more significant. That "something" might be a heavy clamp, tightly bolted to the pipe adjacent to the elbow, or a vessel nozzle, a pump nozzle, a valve, or a flange.

For "flanges" attached to one or both ends, the Code [see footnote 3, Fig. NC-3673.2(b)-1] gives

$$k = 1.65/h^{5/6} \geq 1.0 \text{ for one end flanged} , \quad (7)$$

$$k = 1.65/h^{2/3} \geq 1.0 \text{ for both ends flanged} . \quad (8)$$

Flexibility factors obtained by Eqs. (1), (7), and (8) are shown in Table 1.

Equations (7) and (8) were based on test data given by Pardue and Vigness.[7] In recent years, several authors have published additional data on the effect of flanges attached at the ends of elbows. In particular, Whatham[8] and Thompson and Spence[9] have developed theories applicable to elbows with flanged ends subjected to in-plane moments. Comparisons of their results with Eqs. (1) and (8) are shown in Table 2.

Table 1. Flexibility factors as influenced by end effects

Size	t	R	$h = tR/r^2$	k		
				No flanges [Eq. (1)]	One flange [Eq. (7)]	Two flanges [Eq. (8)]
4	0.237	6	0.313	5.27	4.34	3.58
12	0.375	18	0.176	9.36	7.01	5.25
30	0.375	45	0.0769	21.45	13.99	9.12

Table 2. Influence of end effects on flexibility factors: Comparison with other studies

Size	t	R	h	k			
				No flanges Eq. (1)	Two flanges Eq. (8)	Whatham[a]	Thompson and Spence[b]
4	0.237	6	0.313	5.27	3.58	2.0	2.0
12	0.375	18	0.176	9.36	5.25	2.6	2.2
30	0.375	45	0.0769	21.45	9.12	2.9	2.6

[a]See Ref. 8.

[b]See Ref. 9.

The theoretical values for k are significantly lower than those given by Eq. (8), particularly for small h. In addition, as might be expected intuitively, the theories show that k depends on the elbow angle α and R/r in addition to h.

Another facet of end effects is illustrated when two 90° elbows are welded to each other to produce an S shape, a not uncommon configuration in piping systems. When such a configuration is subjected to in-plane moments, the tendencies for the elbows to ovalize oppose each other at the juncture. This also occurs for an out-of-plane moment at the juncture (torsion at both ends). It, thus, seems reasonable to speculate that the flexibility of the elbows is much like that of a flanged-at-one-end elbow.

3.5 Static Loading Examples

Data presented to this point indicate that elbow flexibilities may be drastically reduced by end effects (e.g., from 21.45 to about 3). However, the effect of this uncertainty in elbow flexibility on supports of a piping system will depend on the details of the piping system. This interaction is illustrated by some simple examples using the configuration shown in Fig. 4(*a*).

Table 3 shows calculated* support loads (F_x, F_y, M_2, and M_1) for several pipe sizes and lengths L_1 and L_2. The loads are for restraint of thermal expansion resulting from an increase in pipe temperature from 70 to 500°F ($\Delta T = 430$°F) for pipe material having a coefficient of thermal expansion of 7.02×10^{-6} in./in./°F. These specific assumptions provide a basis for giving the support forces in pounds and support moments in in.-kips (1000 in.-lb). However, the ratios of the support loads (which we are mainly interested in) would remain the same for any other ΔT or coefficient of thermal expansion. The $k = 2.0$ used in Table 3 is intended to represent the maximum end effects. This might occur if both ends are restrained, for example, in the context of the model of Fig. 4(*a*), by heavy clamps at both ends of the elbow.

Examples 1 through 4 in Table 3 are intended to represent typical proportions of straight pipe to elbows in piping systems. The leg lengths L_1 and L_2 are either 20 or 10 times the nominal size. Example 5 is included to illustrate the effect of increasing the proportion of straight pipe to elbows. Example 6 is the opposite of Example 5 in that the system is all elbow.

The ratio of calculated support loads using $k = 2.0$ to those using k calculated by Eq. (1) varies from 10.7 (Example 6 in Table 1) to 1.09 (Example 1, M_2). Example 6 is a double upper bound of the ratios in that $k = 2.0$ is a maximum possible end effect and the system is all elbow. Examples 1 through 4 are judged to be more representative. For these, the support load ratios vary from 2.7 (Example 3, F_y) to 1.09 (Example 1, M_2).

It may be observed in Table 3 that support loads decrease as the flexibility factor increases. However, this should not be assumed to always be true for static loading. Figure 5 shows simple examples in which increasing the flexibility of one portion of a "piping system" increases the support loads at another portion of the system.

---

*The calculation method is described in Appendix B.

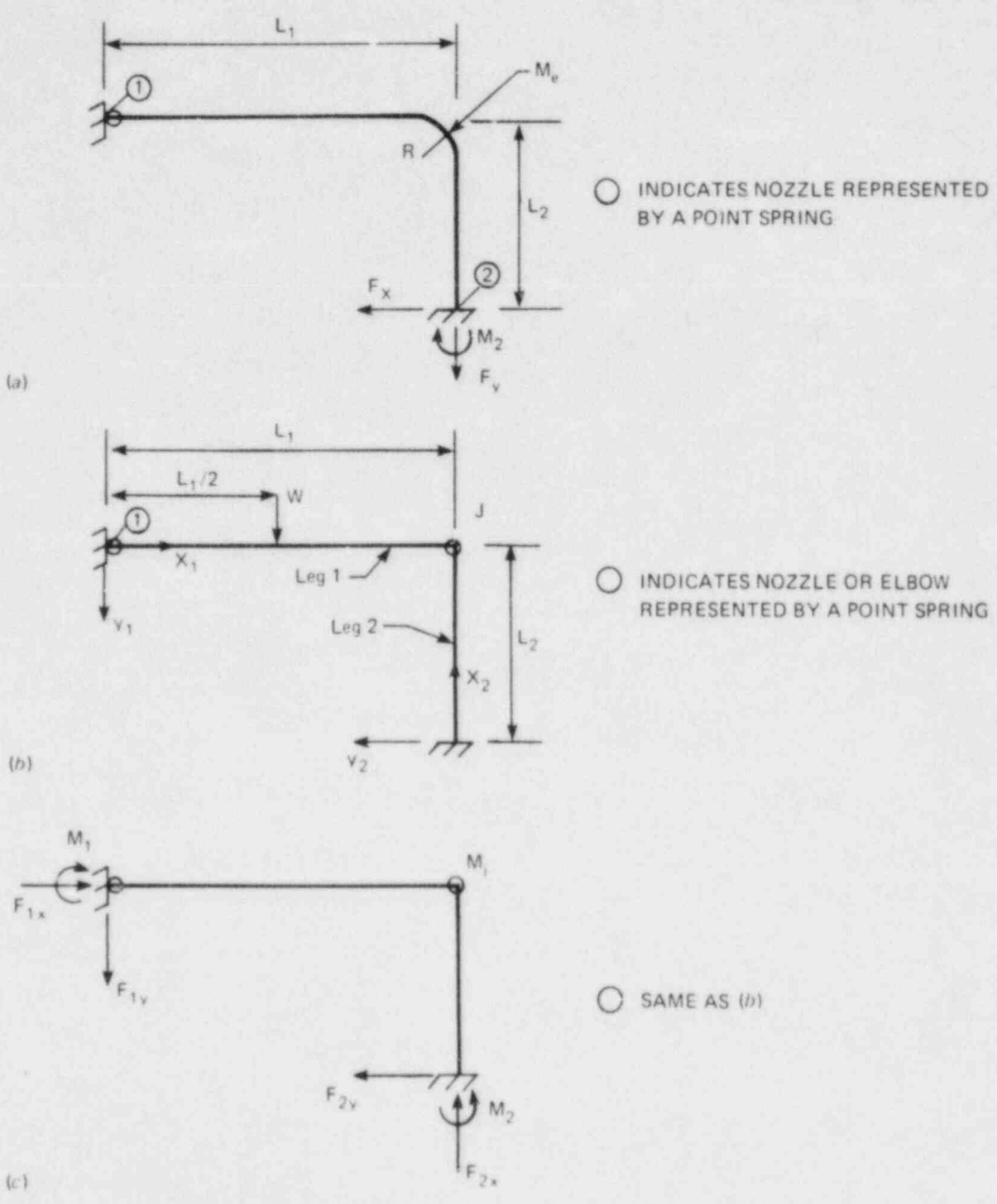

Fig. 4. Configuration used in examples. (*a*) Static-load model; (*b*) dynamic-load model; and (*c*) dynamic-load model support loads and elbow moment M_j.

Table 3. Examples of effect of elbow flexibility on support loads, static loading[a]

Example No.	Pipe size[b]	L_1[c] (in.)	L_2[c] (in.)	R[c] (in.)	k[d]	F_x[a] (lb)	F_y[a] (lb)	M_2[a] (in.-kip)	M_1[a] (in.-kip)	M_e[a] (in.-kip)
1	4	80	40	6	2.00	4,880	−1,420	−127	−45.9	56.5
					5.27	3,990	−960	−117	−34.2	33.9
2	12	240	120	18	2.00	20,900	−6,100	−1640	−591	729
					9.36	15,300	−3,160	−1440	−368	293
3	30	600	300	45	2.00	45,900	−13,400	−9000	−3240	4000
					21.45	29,200	−4,900	−7460	−1650	842
4	30	300	300	45	2.00	39,300	−39,300	−6200	−6200	4550
					21.45	18,900	−18,900	−4380	−4380	783
5	30	6000	3000	45	2.00	479	−145	−909	−344	518
					21.45	383	−97.1	−815	−248	328
6	30	45	45	45	2.00	6,560[e]	−6,560[e]	−80.6[e]	−80.6[e]	41.6[e]
					21.45	611[e]	−611[e]	−7.52[e]	−7.52[e]	3.88[e]

[a]See Fig. 4(*a*) for definition of support loads and elbow moment M_e. This example is for restraint of thermal expansion of 0.003019 in./in., corresponding to an increase in temperature from 70 to 500°F of carbon steel piping.

[b]t = 0.237 in. for 4-in. size; t = 0.375 in. for all other sizes.

[c]See Fig. 4(*a*) for definitions of L_1, L_2, and R.

[d]The second k in each example is from Eq. (1).

[e]Loads divided by 1000.

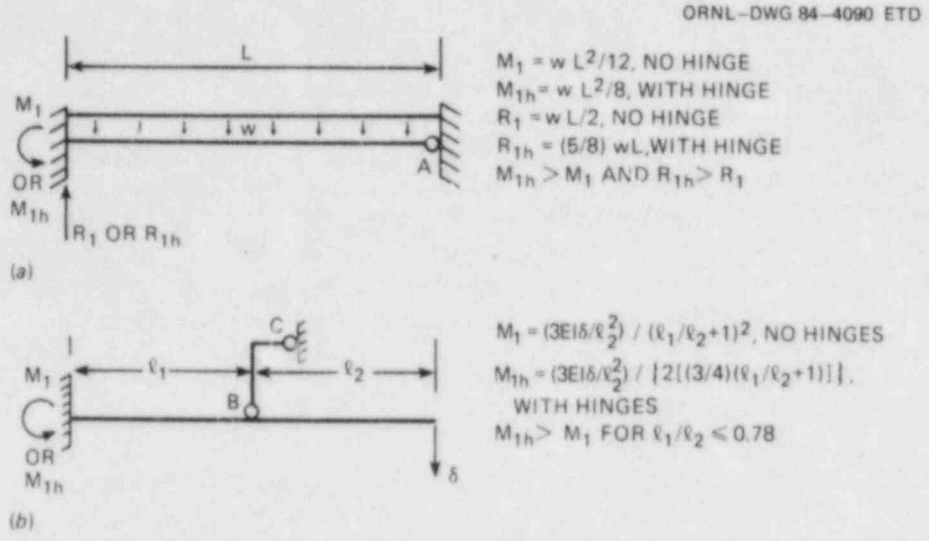

Fig. 5. Simple illustrations of possibility that increasing flexibility of part of piping system may increase support load at another location of piping system. (*a*) Distributed load w(lb/in.), A = hinge location; (*b*) prescribed displacement δ; B, C = hinge locations.

3.6 Dynamic-Loading Examples

The configuration in Fig. 4(*b*) was used to develop some simple examples showing the effect of elbow flexibility on support loads with a simple type of dynamic load. Development of the applicable theory is described in Appendix A. The dynamic load consists of the sudden application of a load W at the location shown in Fig. 4(*b*). The load is then maintained constant. This loading is somewhat like a safety-valve thrust force on a piping system. However, the main motivation in selecting this particular dynamic loading was its relative simplicity.

In the dynamic analysis, the elbow flexibility factor is embodied in the parameter

$$\gamma = (\pi/2)(a_n L_1)(R/L_1)k \ , \qquad (9)$$

where

$a_n L_1 = (m w_n^2/EI)^{1/4} L_1$,
m = mass of pipe per unit length,
w_n = modal frequency,
E = modulus of elasticity,
I = moment of inertia,
L_1 = length of leg 1 [see Fig. 4(*b*)],
R = bend radius of elbow,
k = flexibility factor of elbow [see Eqs. (1) and (3)].

Table 4 gives results of the dynamic analyses for $L_1 = L_2$, and Table 5 gives results for $L_1 = L_2/2$.

The analysis gives the values of a_nL_1 and a_nL_2 shown in Tables 4 and 5. These values are independent of the specific type of dynamic loading. It can be seen in Table 4 that, for $L_1 = L_2$, the first, third, and fifth modes do not depend on the elbow flexibility. This is because the modal shapes are characterized by $y_1 = -y_2$. The elbow does not carry any moment; this is indicated in Table 4 by the column headed M_j/WL_1.

The second and fourth modes *are* dependent on elbow flexibility, as indicated by the results for $\gamma = 0$, 1, and 10. Noting that w_n, the modal frequency, is proportional to a_n^2 and, thus, to $(a_nL_1)^2$, it can be seen that elbow flexibility produces a change in w_n. This, of course, is significant in evaluating earthquake loadings because the dynamic input is frequency dependent (see Fig. 2).

The generalized results can be related to specific dimensions as illustrated by the following example in which $L_1 = L_2 = 600$ in. for 30-in. NPS pipe with 0.375 in. wall and a long-radius elbow with R = 45 in. The value of k derived by Eq. (1) is 21.45, but we want to see what happens if the actual flexibility factor were 2 (e.g., as a result of end effects). For the second mode, using Eq. (9) in which $a_nL_1 = 1.281\pi$ and $k = 21.45$ gives

$$\gamma = (\pi/2)(1.281\pi)(45/600)(21.45) = 10.17 .$$

Using Eq. (9) in which $a_nL_1 = 1.402\pi$, $k = 2$ gives

$$\gamma = (\pi/2)(1.402\pi)(45/600)(2) = 1.04 .$$

The values of γ from Eq. (9) are not exactly the same as those values in Table 4 used to determine the values of a_nL_1. For improved accuracy, one could interpolate the values given in Table 4 and iterate to find corresponding values of γ and a_nL_1, for a specific value of k. Alternatively, one could use the theory of Appendix A and iterate to find corresponding values of γ and a_nL_1. However, for the purpose here, the correspondence is adequate. Accordingly, for this example, decreasing the flexibility factor from 21.45 to 2 increases the second mode frequency by a factor of $(1.40/1.28)^2 = 1.20$. This is a bit larger uncertainty than covered by the practice of peak broadening by ±15% (see Fig. 2). The example constitutes an extreme case in flexibility factor uncertainty and, in most piping systems, the peak broadening could be expected to encompass the uncertainties in elbow flexibilities. However, peak broadening is usually considered to represent uncertainties in developing the response spectra from the ground motion through the building structure to the piping system support locations. From this viewpoint, uncertainties in piping system natural frequencies would conceptually entail additional peak broadening.

Table 4. Examples of elbow flexibility on support loads, dynamic loading,[a] $L_1 = L_2$

Mode	γ[b]	$a_n L_1/\pi$	$a_n L_2/\pi$	$[q(x)]_f$[c]	Q[c]	M_1/WL_1	M_2/WL_1	F_{1y}/W	F_{2y}/W	F_{1x}/W	F_{2x}/W	M_j/WL_1
1	Any	1.250	1.250	−1.445	2.00	−0.187	0.187	0.735	−0.735	0.506	−0.506	0
2	0	1.505	1.505	−1.588	2.00	−0.142	−0.142	0.661	0.661	−0.661	−0.661	−0.142
2	1	1.402	1.402	−1.564	2.09	−0.154	−0.154	0.668	0.668	−0.632	−0.632	−0.0982
2	10	1.281	1.281	−1.477	2.04	−0.179	−0.179	0.718	0.718	−0.541	−0.541	−0.0240
3	Any	2.250	2.250	−0.5704	2.00	−0.0228	0.0228	0.161	−0.161	−0.114	0.114	0
4	0	2.500	2.500	0.000557	2.00	0.0000	0.0000	−0.0001	−0.0001	−0.0001	−0.0001	0.0000
4	1	2.397	2.397	−0.2360	2.05	−0.0081	−0.0081	0.0612	0.0612	0.0581	0.0581	0.0051
4	10	2.278	2.278	−0.5076	2.02	−0.0195	−0.0195	0.140	0.140	0.108	0.108	0.0024
5	Any	3.250	3.250	1.300	2.00	0.0249	−0.0249	−0.255	0.255	−0.179	0.179	0

[a] Load W suddenly applied at point shown in Fig. 4(*b*) and maintained constant.

[b] $\gamma = (\pi/2)\ (a_n L_1)\ (R/L_1)k$, where k = elbow flexibility factor.

[c] See Appendix A for significance of these parameters.

Table 5. Examples of elbow flexibility on support loads, dynamic loading,[a] $L_1 = L_2/2$

Mode	γ[b]	$a_n L_1/\pi$	$a_n L_2/\pi$	$[q(x)]_f$[c]	σ[c]	M_1/WL_1	M_2/WL_1	F_{1y}/W	F_{2y}/W	F_{1x}/W	F_{2x}/W	M_j/WL_1
1	0	0.696	1.392	−0.5801	17.6	−0.0276	0.0799	0.0857	−0.171	0.160	0.0606	0.0479
1	1	0.665	1.330	−0.5322	57.4	−0.0085	0.0445	0.0263	−0.0921	0.0780	0.0198	0.0151
1	10	0.6326	1.2652	−0.4837	1540	−0.0003	0.0088	0.0010	−0.0175	0.0126	0.0008	0.0006
2	0	1.15372	2.30744	−1.327	6.22	−0.0650	−0.105	0.241	0.381	0.314	−0.107	0.0267
2	1	1.147	2.294	−1.317	11.4	−0.0356	−0.0307	0.132	0.291	0.233	−0.0558	0.0156
2	10	1.1314	2.2628	−1.295	158	−0.0026	−0.0229	0.0095	0.0814	0.0599	−0.0036	0.0013
3	0	1.395	2.790	−1.560	1.37	−0.237	0.103	1.025	−0.448	−0.275	−0.963	−0.144
3	1	1.336	2.672	−1.524	1.18	−0.293	0.0806	1.215	−0.338	−0.290	−1.040	−0.108
3	10	1.2657	2.5314	−1.461	1.02	−0.362	0.0245	1.444	−0.0977	−0.0973	−1.039	−0.0248
4	0	1.704	3.408	−1.500	9.40	−0.0223	−0.0455	0.118	0.244	−0.234	−0.0948	−0.0309
4	1	1.667	3.334	−1.529	28.7	−0.0078	−0.0288	0.0401	0.150	−0.130	−0.0348	−0.0105
4	10	1.6324	3.2648	−1.552	801	−0.0003	−0.0059	0.0015	0.0301	−0.0223	−0.0014	−0.0004
5	0	2.155	4.310	−0.7776	5.99	−0.0113	0.0178	0.0766	−0.120	−0.0996	0.0369	−0.0047
5	1	2.147	4.294	−0.7940	10.9	−0.0064	0.0143	0.0431	−0.0964	−0.0768	0.0193	−0.0029
5	10	2.1315	4.253	−0.8271	161	−0.0005	0.0041	0.0031	−0.0274	−0.0202	0.0012	−0.0002

[a] Load suddenly applied at point shown in Fig. 4(b) and maintained constant.

[b] $\gamma = (\pi/2)\ (a_n L_1)\ (R/L_1)k$, where k = elbow flexibility factor.

[c] See Appendix A for significance of these parameters.

The total support loads can be obtained by summing the loads for each mode. Continuing with the 30-in. by 0.375-in. pipe and elbow example for which $L_1 = L_2 = 600$ in., M_1/WL_1 is $(-0.187 - 0.154 - 0.0228 - 0.0081 + 0.0249) = -0.347$ for $\gamma = 1$ ($k = 2$), whereas M_1/WL_1 is $(-0.187 - 0.179 - 0.0228 - 0.0195 + 0.0249) = -0.383$ for $\gamma = 10$ ($k = 21.45$). Considering the drastic assumption regarding the change in k, this is a very small change in the support load M_1.

The cognizant reader will be aware that Tables 4 and 5 include only the first five modes and that higher modes could change the total support loads. Also, as discussed in Appendix A, data on loads from Tables 4 and 5 may be subject to rounding errors and inaccuracies in the numerical integration technique used. However, the particular dynamic loading example was selected (in part) because the total support loads can be obtained from a static analysis, using a dynamic load factor of 2.0.

Table 6 summarizes the bounds derived from the static analysis of the configuration shown in Fig. 4(*b*). The first two lines of the two groups of data in which $L_2/L_1 = 1.0$ and $L_2/L_1 = 2.00$ show the bounds of support loads for Tables 4 and 5, respectively. (The third line of each group and the last two groups in Table 6 will be discussed in Sect. 4.)

It can be seen in Table 6 that, even at the bounds, the change in M_1 is small. Large percentage changes might occur in M_2, F_{2y}, and F_{1x}, but these loads are small compared with M_1, F_{1y}, and F_{2x}; hence, the effect on the adequate design of supports for calculated loads would be small. This, of course, cannot be generalized, even for the same type of loading, but where $L_2/L_1 = 0.25$, it is apparent from Table 6 that F_{2y} and F_{1x} can become dominant support forces and could change significantly with the elbow flexibility.

As mentioned previously in Sect. 3.5, Table 6 shows examples in which an increase in the flexibility of part of a piping system will increase the support loads. Accordingly, in general, it is impossible to define a "conservative" elbow flexibility factor either for static or dynamic loads. A sensitivity study is needed to establish the parameters (e.g., ratio of straight pipe lengths to elbow lengths) where elbow flexibility is significant with respect to support loads. The results given in Tables 3, 4, and 5 represent an initial step toward this objective.

Table 6. Bounding solutions[a] to dynamic loading examples, static analysis with dynamic load factor of 2.0

L_2/L_1[b]	γ[c]	γ_b[d]	$-M_1/WL_1$	$-M_2/WL_1$	F_{1y}/W	F_{2y}/W	F_{1x}/W	F_{2x}/W	M_j/WL_1
1	0	0	−0.3125	0.0625	1.1875	−0.1875	−0.1875	−0.8125	−0.1250
	∞	0	−0.3750	0	1.375	0	0	−0.625	0
	0	∞	0	0.1071	0.7857	−0.3214	−0.3214	−1.2143	−0.2143
2	0	0	−0.3333	0.0417	1.250	−0.0625	−0.0625	−0.7500	−0.08333
	∞	0	−0.3750	0	1.375	0	0	−0.6250	0
	0	∞	0	0.0750	0.850	−0.1125	−0.1125	−1.1500	−0.1500
0.5	0	0	−0.2917	0.0833	1.125	−0.500	−0.500	−0.875	−0.1667
	∞	0	−0.3750	0	1.375	0	0	−0.625	0
	0	∞	0	0.1364	0.7273	−0.8181	−0.8181	−1.2727	−0.2727
0.25	0	0	−0.2750	0.100	1.075	−1.200	−1.200	−0.925	−0.2000
	∞	0	−0.3750	0	1.375	0	0	−0.625	0
	0	∞	0	0.1579	0.6842	−1.8947	−1.8947	−1.3158	−0.3158

[a] See Fig. 4(*b* and *c*). Support loads are those applied to the supports by the piping.

[b] See Fig. 4(*b*).

[c] $\gamma = (\pi/2)\ (a_n/L_1)\ (R/L_1)k$, where k = elbow flexibility factor.

[d] $\gamma_b = (a_n L_1)k_b\ d/L_1$, where k_b = nozzle flexibility factor.

4. NOZZLE FLEXIBILITY

4.1 Available Data on Nozzle Flexibility

Flexibility of nozzles is usually not considered in a piping system analysis, even though there is some (nonmandatory) guidance in NB-3686.5 by the equations

$$k = 0.1(D/T)^{3/2}[(T/t_n)(d/D)]^{1/2}(t/T) \text{ for } M_{x3} , \tag{10}$$

$$k = 0.2(D/T)[(T/t_n)(d/D)]^{1/2}(t/T) \text{ for } M_{z3} , \tag{11}$$

$$\phi = kMd/EI_b . \tag{12}$$

(The nomenclature used in Eqs. (10), (11), and (12) is given in Fig. 6.)

Equations (10) through (12) were developed by Rodabaugh and Moore.[10] They are based on correlations with finite-element analysis and available test data and are intended to be applicable to fabricated branch connections with $D/T \leq 100$ and $d/D \leq 0.5$.

As indicated in Fig. 6, the flexibility of a nozzle is intended to be used in a piping system analysis as a point-spring at the surface of the vessel or run pipe. The value of k gives the ratio of the rotation of the point-spring to the rotation of a one-diameter length of branch pipe. When the value of k is so expressed, it has an immediate significance. If k is small compared to the length (in diameters) of pipe attached to the nozzle, then the nozzle flexibility will have little influence on support loads. Conversely, if k is large compared to the attached pipe length, the nozzle flexibility may have a large influence on support loads. Examples are given in Sects. 4.3 and 4.4.

Equations (10) and (11) were developed for piping for which D/T seldom exceeds 100. Steele[11] gives data that are applicable to larger values of D/T. His data are significant because a piping system may be attached to a nozzle in a thin-wall tank with $D/T \gg 100$. As will become apparent, ignoring the nozzle flexibility in thin-wall tanks can lead to gross errors in calculated support loads.

Steele[11] gives data on the flexibility of a rigid cross-section (plug) nozzle in the form of a graph of $M/ET^3\phi^0$ as a function of λ, where M is either M_{x3} or M_{z3}, ϕ^0 is the rotation in degrees, and $\lambda = (d/D)\sqrt{D/T}$. That data can be used to calculate a flexibility factor for the nozzle by

$$\phi = (\pi/180)\ \{M/[ET^3 f(\lambda)]\} , \tag{13}$$

where $f(\lambda) = (M/ET^3\phi^0)$ for a particular value of λ. Equation (13) can be written as

$$\phi = \frac{Md}{E(\pi d^3 t/8)} \left[\frac{\pi^2}{8 \times 180}\left(\frac{D}{T}\right)^2 \left(\frac{d}{D}\right)^2 \frac{t}{T} \frac{1}{f(\lambda)}\right] , \tag{14}$$

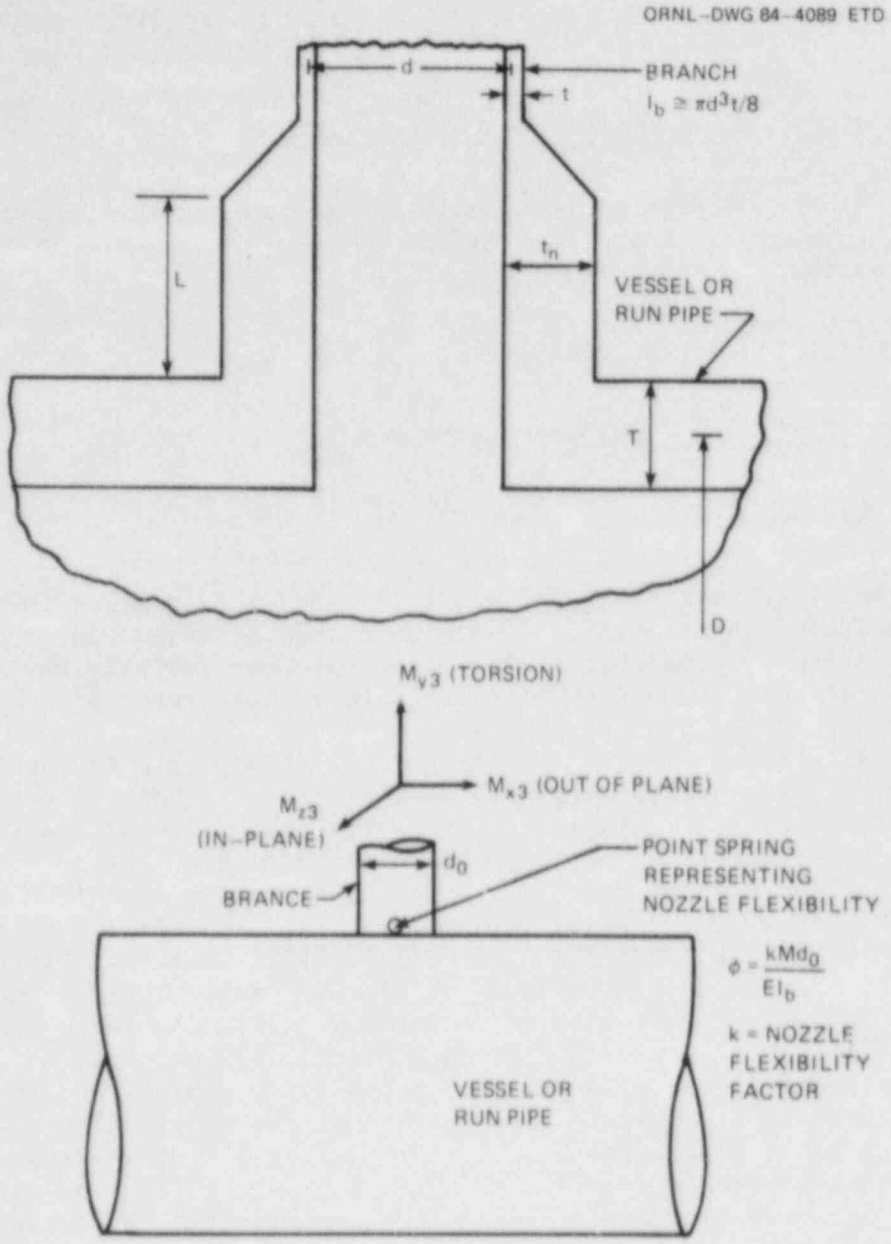

Fig. 6. Nozzle terminology.

and k is the quantity in brackets. In developing Eq. (14) from Eqs. (12) and (13), the approximation $I_b = \pi d^3 t/8$ was used. Of course, because the Steele[11] data are for a "plug" nozzle, the introduction of (t/T) in k is simply to express the flexibility of a plug nozzle in terms of a nozzle with a given (t/T).

Table 7 shows the available test data on nozzle flexibility[12-18] and comparisons with Eqs. (10) and (11), headed Code, and with Eq. (14), headed Ref. 11. In converting measured rotations to k-factors, E was

Table 7. Test data on flexibility of nozzles and comparisons with Eqs. (10), (11), and (14)

Ref. No.[a]	D/T	d/D	t/T[b]	Out-of-plane moment, k_{x3}			In-plane moment, k_{z3}		
				Test[c]	Code[d]	Ref. 11[e]	Test[c]	Code[f]	Ref. 11[g]
12	76	0.18	0.76	31	24.5	26 44	17	5.62	2.8
13	78	0.13	0.45	11	16.7	12 19	5.6	3.77	3.2
14	93	0.12	0.42	10	20.1	14 21	4.0	4.18	3.6
14	93	0.18	0.75	27	33.0	33 63	8.0	6.83	-
15	1050	0.011	0.63	52	283	52 64	32	17.5	32
15	1050	0.028	1.09	310	594	310 450	140	36.7	120
16, 17	2530	0.010	0.53	140	926	180 220	58	36.8	93
16	2530	0.050	0.53	1200	2070	690 1800	240	82.4	-
18	960	0.0042	1.00	64	193	16 18	51	12.4	11

[a] See Sect. 10 for references.

[b] $t = t_n$ for all specimens.

[c] Carbon steel test specimens tested at room temperature; $E = 3 \times 10^7$ psi used in obtaining values for k from measured rotations.

[d] Equation (10).

[e] Equation (14); the first value is for $\Lambda = 14$; second value is for $\Lambda = \infty$.

[f] Equation (11).

[g] Equation (14); not dependent on Λ.

taken as 3×10^7 psi. All test specimens were made of carbon steel material and were tested at room temperature. In all specimens, the branch pipe was long enough to be effectively of infinite length and, in all specimens, $t = t_n$.

For M_{x3} (out-of-plane moment) Steele[11] gives $M/ET^3\phi^0$ as a function of λ for $\Lambda = 14$, 50, 100, and ∞; where $\Lambda = L/\sqrt{DT}$, and L is the length of the vessel. The data are based on a thin-shell analysis of a cylindrical shell with "simple support at the ends of the cylinder." Table 7 shows k_{x3} for $\Lambda = 14$ and ∞. Steele[11] covers λ only up to 1.5 for M_{z3}, hence, the dashes in Table 7 for specimens in which $\lambda > 1.5$. Only one curve for M_{z3} (labeled $\Lambda = 14$) is given, and the observation that $M_{z3}/ET^3\phi^0$ has "a very weak dependence on the cylinder length" is made.

Examination of Table 7 indicates that the Code equations, when extrapolated to D/T >> 100, tend to overestimate k_{x3} and underestimate k_{z3}. Results of Steele[11] for k_{x3}, based on $\Lambda = 14$, are in reasonable agreement with the tests, but results for k_{z3} tend to be more erratic with respect to test data. It should be noted that the experimental determination of flexibility of nozzles in vessels or run pipe requires an appropriate reference frame for mounting dial gages to measure rotation, accurate control of the moment load, and accurate displacement readings. Some of the discrepancies apparent in Table 7 may be the result of inadequate experimental techniques.

Table 8 shows comparisons of nozzle flexibility factors obtained by finite element analyses (FEA) with Eqs. (10) and (11), the Code equations, and Eq. (14), headed Ref. (11). Dashes are inserted where data from Steele[11] do not cover the model (i.e., for $\lambda > 1.5$ for M_{z3} and for $\lambda > 3$ for M_{x3}, $\Lambda = 14$).

The first group of six models are essentially unreinforced with respect to a pressure that fully utilizes the vessel or run-pipe wall thickness. In these models, $t/T = t_n/T = d/D$. The second group of 14 models

Table 8. Finite-element analysis (FEA) data on flexibility of nozzles and comparisons with Eqs. (10), (11), and (14)

D/T	d/D and t/T	t_n/T	Out-of-plane moment k_{x3}				In-plane moment k_{z3}		
			FEA	Code, Eq. (10)	Ref. 11, Eq. (14)		FEA	Code, Eq. (11)	Ref. 11, Eq. (14)
					$\Lambda = 14$	$\Lambda = \infty$			
102	0.5	0.5	47.0	51.5	-	150	8.89	10.2	-
82	0.5	0.5	37.2	37.1	-	100	7.68	8.2	-
42	0.5	0.5	16.2	13.6	-	38	4.58	4.2	-
22	0.5	0.5	6.92	5.16	6.4	15	2.65	2.2	-
12	0.5	0.5	2.84	2.08	2.9	5.4	1.50	1.2	-
12	0.08	0.08	1.96	0.33	0.052	0.062	1.91	0.19	0.034
102	0.5	4.34	17.8	17.5	-	150	2.70	3.46	-
82	0.5	4.01	14.5	13.1	-	100	2.42	2.90	-
42	0.5	3.14	6.32	5.43	-	38	1.46	1.68	-
22	0.5	2.45	2.33	2.33	15	6.4	0.72	0.99	-
12	0.5	1.92	0.69	1.06	2.9	5.4	0.24	0.61	-
42	0.32	2.56	4.07	3.08	7.1	15	1.09	0.95	-
22	0.32	1.98	1.41	1.32	3.1	5.2	0.49	0.57	0.42
12	0.32	1.52	0.33	0.61	1.3	1.9	0.07	0.35	0.35
42	0.16	1.88	2.11	1.27	2.2	3.1	1.14	0.39	0.62
22	0.16	1.43	0.95	0.55	0.78	1.0	0.71	0.24	0.33
12	0.16	1.08	0.35	0.26	0.29	0.37	0.28	0.15	0.14
42	0.08	1.38	2.02	0.52	0.47	0.56	1.85	0.16	0.22
22	0.08	1.03	1.43	0.23	0.15	0.18	1.39	0.10	0.092
12	0.08	0.72	0.81	0.11	0.052	0.062	0.80	0.06	0.034

is fully reinforced with respect to a pressure that fully utilizes the vessel or run-pipe wall thickness. The reinforcing is in accordance with the rules of NB-3640, with reinforcement shape as indicated in Fig. 6.

Because the Steele[11] data are for plug nozzles, the values of k derived from them are independent of t_n/T for a given t/T. In this respect, the data are notably inconsistent with both the finite-element analysis and the Code equations. There are other inconsistencies in the comparisons (e.g., the sixth model for which the finite-element analysis gives $k_{x3} = 1.96$ as compared with the Code $k_{x3} = 0.33$ and the Steele[11] $k_{x3} = 0.05$ or 0.06).

Although there are inconsistencies in the available data and more work is needed to accurately quantify flexibility of nozzles, two general aspects are apparent.

1. For vessels or run pipe having small D/T, such as reactor pressure vessels and the connected pipe, k_{x3} and k_{z3} are small and will have little influence on calculated support loads.
2. For vessels or run pipe having large D/T, k_{x3} and k_{z3} may be large and may have a significant influence on calculated support loads.

The third moment M_{y3} is a torsional moment on the nozzle. For small d/D, one could speculate that k_{y3} would be close to unity. However, we do not have any data to support that speculation.

Further study is obviously needed to establish the parameters where nozzle flexibility is significant with respect to support loads (e.g., ratio of nozzle flexibility factor to length of piping). The results given later in Sects. 4.3 and 4.4 represent an initial step toward this objective.

4.2 Representative Values of k_{x3} and k_{z3}

Table 9 shows representative values of k_{x3} and k_{z3} that might be encountered in piping systems. Typically, piping (or branch pipes in fabricated branch connections) tend to have a lower d/t than the D/T of the vessel or run pipe. The set of k values in Table 9 headed $t/T = t_n/T = 2d/D$ represent such nozzles. Conceptually, the branch pipe is welded directly to the vessel or run pipe without any local thickening at the vessel or run pipe. Such nozzles always meet Code reinforcing requirements for *some* design pressure, which is roughly one-half of the maximum allowable pressure for the unperforated vessel or run pipe. The Code-required reinforcement comes from excess thickness in the vessel or run-pipe wall.

The other set of k values in Table 9 are for configurations like Fig. 6 with t_n/T such that the following equation is met:

$$dT = 2L[t_n - (d/D)T] \quad . \tag{15}$$

Table 9. Representative values of nozzle flexibility factors k_{x3} and k_{z3}

D/T	d/D	t/T = t_n/T = 2 d/D				t/T = 2 d/D		
		k_{x3}		k_{z3}		t_n/T[d]	k_{x3} Code, Eq. (10)	k_{z3} Code, Eq. (11)
		Code[a]	Ref. 11[b]	Code[c]	Ref. 11[b]			
10	0.05	0.224	0.026	0.141	0.016	1.034	0.070	0.044
	0.10	0.447	0.16	0.283	0.083	1.324	0.174	0.110
	0.20	0.894	0.91	0.566	0.33	1.723	0.431	0.273
	0.50	2.24	7.97	1.41	0.49	2.700	1.41	0.894
50	0.05	2.50	0.47	0.707	0.24	1.741	0.600	0.169
	0.10	5.00	2.66	1.41	0.90	2.223	1.50	0.424
	0.20	10.0	13.7	2.83	1.31	2.848	3.75	1.06
	0.50	25.0	99.6	7.07		4.027	12.5	3.52
100	0.01	1.41	0.024	0.283	0.016	1.270	0.177	0.035
	0.02	2.83	0.15	0.566	0.091	1.598	0.447	0.089
	0.05	7.07	1.63	1.41	0.70	2.191	1.51	0.302
	0.10	14.1	8.84	2.83	1.96	2.785	3.79	0.760
	0.20	28.3	42.2	5.66		3.551	9.49	1.90
	0.50	70.7	296	14.1		4.980	31.7	6.40
500	0.01	15.8	0.46	1.41	0.26	2.160	1.52	0.136
	0.02	31.6	2.74	2.83	1.25	2.730	3.83	0.342
	0.05	79.1	25.2	7.07	4.66	3.715	13.0	1.16
	0.10	158	122	14.1		4.707	32.6	2.92
1000	0.01	44.7	1.61	2.83	0.83	2.723	3.83	0.242
	0.02	89.4	9.14	5.66	3.32	3.434	9.65	0.611
	0.05	224	79.7	14.1	4.90	4.676	32.7	2.07
	0.10	447	351	28.3		5.918	82.2	5.20

[a] Equation (10) gives $k_{x3} = 0.1\ (D/T)^{3/2}\ (d/D) \times \sqrt{2}$.

[b] Equation (14); for M_{x3}, $f(\lambda)$ is for $\lambda = \infty$; values of k do not depend on t_n/T.

[c] Equation (11) gives $k_{z3} = 0.2\ (D/T)\ (d/D) \times \sqrt{2}$.

[d] t_n/T obtained from Eq. (15).

The nozzle length L is taken as $0.5\sqrt{dt_n/2}$, the length of countable reinforcement in NB-3640 (with $r_2 = 0$). These k values are representative of nozzles in vessels where all the Code-required reinforcement comes from extra thickness in the nozzle.

Table 9 indicates k values ranging from near zero, where the nozzle is essentially an anchor, to 447, where the nozzle is almost a hinge. Values of D/T up to 100 and d/D up to 0.5 are applicable to branch connections in piping. Values of D/T of 500 and 1000 are applicable to large, low-pressure storage tanks; a d/D of 0.10 is about an upper bound for piping to such tanks.

It is pertinent to bring out another aspect of k-factors using, as an example, a tank with D/T = 1000, d/D = 0.048, $t/T = t_n/T = 2d/D = 0.096$. Let us assume that D = 375 in. and T = 0.375 in. Then d = 0.048 × 375 = 18 in. and $t = t_n = 0.036$ in. Now, carbon steel pipe is normally available in standard weight; for 18-in. pipe, the wall thickness is

0.375 in. The 18-in. pipe attached to this tank is much more likely to have $t = t_n = 0.375$ in. than 0.036 in. However, in that case, $t_n/T = t/T = 1.00$ and Eq. (10) gives $k_{x3} = 693$, whereas Eq. (14), for $\Lambda = \infty$, gives $k_{x3} = 752$.

Accordingly, for the purpose of assessing the influence of nozzle flexibility on support loads, we are interested in values of k ranging from essentially zero to about 1000.

4.3 Static-Loading Examples

The effect of nozzle flexibility on support loads is illustrated in Table 10, using the configuration shown in Fig. 4(*a*). The nozzle flexibility factor is identified as k_b to distinguish it from the elbow flexibility factor k.

If the piping is anchored to a thick-wall vessel or if d/D is small, the nozzle flexibility will be small and little error will be caused by assuming a nozzle flexibility of zero. However, if (1) the piping is anchored to a thin-wall vessel, (2) an out-of-plane moment is a major loading, and (3) it is assumed that the nozzle flexibility is zero, gross overestimates of the loads at the nozzle will be calculated.

As a specific example, for a vessel having D = 255 in. and T = 0.375 in., and for which the 12.75-in.-OD × 0.375-in.-wall branch is "stubbed-in" without additional reinforcement D/T = 680, d/D = 0.05, and $t_n/T = t/T = 1.00$. Equation (10) gives

$$k_b = 0.1 \times (680)^{3/2} \times (1 \times 0.05)^{1/2} \times 1 = 396 ,$$

and Eq. (14) [for out-of-plane moment, $\Lambda = \infty$, $\lambda = 1.30$, $f(\lambda) = 0.019$] gives

$$k_b = [\pi^2/(8 \times 180)] \times (680)^2 \times (0.05)^2 \times 1/0.019 = 417 .$$

For this example, it can be seen in Table 10 by interpolating between $k_b = 100$ and 1000, that for $k_b = 417$, the moment at the nozzle (M_1) would be overestimated by a factor of around 100 if the nozzle flexibility is ignored.

Overestimating the nozzle loads may be harmful in that it might cause the piping designer to add more restraints or reroute the piping system. This would add to the cost and might result in a less reliable piping system.

As can be seen in Table 10, loads on both the nozzle and the anchor at point 2 decrease with an increase in k_b. However, as discussed in Sects. 3.5 and 3.6, this should not be assumed to be true for all piping systems.

Table 10. Examples of effect of nozzle flexibility on support loads, static loading[a]

L_1[b] (in.)	L_2[b] (in.)	R[b] (in.)	k[c]	k_b[c]	F_x[d] (lb)	F_y[d] (lb)	M_2[d] (in.-kip)	M_1[d] (in.-kip)	M_e[d] (in.-kip)
240	120	18	2.00	0	20,900	−6,100	−1,640	−591	729
				1	20,500	−5,570	−1,620	−496	703
				10	19,300	−3,950	−1,570	−203	622
				100	18,600	−2,990	−1,540	−29.3	574
				1000	18,500	−2,840	−1,540	−3.07	566
			9.36	0	15,300	−3,160	−1,440	−368	293
				1	15,100	−2,900	−1,430	−313	286
				10	14,700	−2,030	−1,410	−134	264
				100	14,400	−1,480	−1,400	−19.9	251
				1000	14,400	−1,390	−1,400	−2.09	248
120	240	18	2.00	0	6,100	−20,900	−591	−1640	729
				1	5,590	−16,700	−550	−1211	674
				10	4,590	−8,280	−469	−362	564
				100	4,210	−5,150	−439	−45.1	524
				1000	4,170	−4,750	−435	−4.63	518
			9.36	0	3,160	−15,300	−368	−1440	293
				1	2,900	−11,900	−346	−1080	272
				10	2,360	−4,960	−299	−329	228
				100	2,150	−2,300	−281	−41.4	211
				1000	2,120	−1,960	−279	−4.25	209

[a]See Fig. 4(*a*) for configuration. Example is for 12-in., standard-weight pipe and elbow.

[b]See Fig. 4(*a*) for definitions of L_1, L_2, and R.

[c]k = elbow flexibility factor, k_b = nozzle flexibility factor.

[d]See Fig. 4(*a*) for definition of support loads and elbow moment M_e. This example is for restraint of thermal expansion of 0.003019 in./in. corresponding to an increase in temperature from 70 to 500°F of carbon steel piping.

4.4 Dynamic-Loading Examples

The configuration and specific dynamic loading used in Sect. 3.6 for elbows was also used for a simple example showing the effect of nozzle flexibility on modal frequencies and support loads. Development of the applicable theory is described in Appendix A.

In the dynamic analysis, the nozzle flexibility factor is embodied in the parameter

$$\gamma_b = (a_n L_1) k_b d/L_1 \ . \tag{16}$$

Table 11 gives modal frequencies and support loads as a function of γ_b. The first three groups are for $L_1 = L_2$, first, second, and third modes, followed by three groups for $L_1 = L_2/2$ and three groups for $L_1 = 2L_2$. The last group is for $L_1 = 4L_2$, first mode only.

For the dimensions used in the static loading example, d = 12.75 in. and $k_b \cong 400$. For $L_x = 240$, $L_y = 120$, and $a_n L_1 = 1.167\pi$ (see Group 7 in Table 11), Eq. (16) gives

$$\gamma_b = (1.167\pi) \times 400 \times 12.75/240 = 78 \ .$$

There is a seemingly large lack of correspondence in using $a_n L_1 = 1.167\pi$ for $\gamma_b = 10$ and the value of $\gamma_b = 78$ for this specific example. However, analogous to the bounding aspect of $\gamma = 10$ for elbow flexibility, increasing γ_b above 10 does not change the modal frequencies significantly. To illustrate this, results for $\gamma_b = 100$ are shown for Group 1 in Table 11. The results for $\gamma_b = 100$ are almost identical to the theoretical solution with the spring representing the nozzle flexibility replaced by a hinge.

Accordingly, for the specific example of D = 255 in., T = 0.375 in., d = 12.75 in., $t = t_n = 0.375$ in., $L_1 = 240$ in., $L_2 = 120$ in., it can be seen in Table 11 for Group 7 that assuming the nozzle flexibility is zero leads to an overestimate in the first-mode frequency by a factor of $(1.392/1.167)^2 = 1.42$.

Noting that the modal frequency w_n is proportional to a_n^2 and, thus, to $(a_n L_1)^2$, it can be seen in Table 11 that the ratios of natural frequencies [$(a_n L_1)^2$, $\gamma_b = 0/(a_n L_1)^2$, and $\gamma_b = 10$] range from 1.42 to 1.03. These represent the overestimate of modal frequencies because the nozzle flexibility is assumed to be zero.

For $\gamma_b = 10$ the nozzle appears to act almost like a hinge; thus, it is informative to calculate values of k_b corresponding to $\gamma_b = 10$. Equation (16) for $\gamma_b = 10$ gives

$$k_b = \frac{10}{(a_n L_1)(d/L_1)} \ . \tag{17}$$

Values of k_b for a representative range of $a_n L_1$ and d/L_1 are presented in Table 12. With values of k_b equal to or larger than the values in Table 12, the nozzle flexibility is sufficient to essentially provide a hinge at the nozzle.

Table 11. Examples of effect of nozzle flexibility on support loads (dynamic loading)[a]

Mode	Group No.	γ_b[b]	$a_n L_1/\pi$	$a_n L_2/\pi$	$[q(x)]_f$[c]	θ[c]	M_1/WL_1	M_2/WL_1	F_{1y}/W	F_{2y}/W	F_{1x}/W	F_{2x}/W	M_j/WL_1
1	1	0	1.250	1.250	−1.445	2.00	−0.187	0.187	0.735	−0.735	0.506	−0.506	0
		0.1	1.235	1.235	−1.628	2.26	−0.191	0.193	0.814	−0.750	0.490	−0.588	−0.013
		1.0	1.1595	1.1595	−3.372	7.24	−0.140	0.200	1.010	−0.745	0.342	−0.915	−0.077
		10.0	1.0925	1.0925	−21.65	274	−0.0269	0.202	0.984	−0.727	0.196	−1.150	−0.133
		100	1.0801	1.0801	−205	22,500	−0.00317	0.221					
2	2	0	1.505	1.505	−1.588	2.00	−0.142	−0.142	0.661	0.661	−0.661	−0.661	−0.142
		0.1	1.4918	1.4918	−1.747	2.68	−0.119	−0.143	0.600	0.659	−0.657	−0.603	−0.137
		1.0	1.447	1.447	−3.273	16.6	−0.0381	−0.129	0.337	0.578	−0.568	−0.364	−0.104
		10	1.424	1.424	−18.96	962	−0.0039	−0.108	0.186	0.474	−0.458	−0.225	−0.0777
3	3	0	2.250	2.250	−0.5704	2.00	−0.0228	0.0228	0.161	−0.161	−0.114	0.114	0
		0.1	2.2349	2.2349	−0.5277	2.25	−0.0190	0.0192	0.147	−0.135	−0.0909	0.109	0.0013
		1.0	2.1602	2.1602	−0.2356	7.26	−0.0028	0.0041	0.0382	−0.0277	−0.0134	0.0352	0.0016
		10	2.0953	2.0953	−2.3026	286	0.0007	−0.0059	−0.0539	0.0387	0.0115	−0.0627	−0.0039
1	4	0	0.696	1.392	−0.5801	17.6	−0.0276	0.0799	0.0857	−0.171	0.160	0.0606	0.0479
		0.1	0.695	1.390	−0.7361	23.3	−0.0265	0.0879	0.0909	−0.189	0.176	0.0601	0.0514
		1.0	0.689	1.378	−2.133	106	−0.0176	0.124	0.111	−0.265	0.242	0.0529	0.0668
		10	0.6848	1.3696	−16.12	4,320	−0.0032	0.144	0.114	−0.306	0.277	0.0341	0.0728
2	5	0	1.15372	2.30744	−1.327	6.22	−0.0650	−0.105	0.241	0.381	0.314	−0.107	0.0267
		0.1	1.1487	2.2974	−1.522	6.57	−0.0710	−0.116	0.287	0.418	0.339	−0.147	0.0244
		1.0	1.1172	2.2344	−3.318	13.9	−0.0774	−0.161	0.541	0.563	0.381	−0.440	−0.0112
		10	1.0764	2.1528	−21.59	392	−0.0193	−0.179	0.699	0.606	0.281	−0.791	−0.0762
3	6	0	1.395	2.790	−1.5604	1.37	−0.237	0.103	1.025	−0.448	−0.275	−0.963	−0.144
		0.1	1.374	2.748	−1.7320	1.52	−0.245	0.122	1.142	−0.526	−0.374	−1.083	−0.172
		1.0	1.2967	2.5934	−3.4309	9.16	−0.0903	0.128	0.713	−0.522	−0.500	−0.788	−0.159
		10	1.2554	2.5108	−21.274	589	−0.0093	0.127	0.383	−0.502	−0.502	−0.530	−0.130
1	7	0	1.392	0.696	−1.559	1.06	−0.307	0.107	1.327	−0.664	−0.469	−1.239	−0.183
		0.1	1.366	0.683	−1.728	1.31	−0.286	0.108	1.330	−0.672	−0.488	−1.252	−0.192
		1.0	1.252	0.626	−3.432	5.44	−0.163	0.125	1.249	−0.764	−0.617	−1.328	−0.227
		10	1.167	0.5835	−21.70	227	−0.0285	0.144	1.097	−0.877	−0.745	−1.441	−0.268
2	8	0	2.30744	1.15372	−0.4410	3.19	−0.0282	−0.0175	0.205	0.130	−0.0574	0.168	0.0072
		0.1	2.283	1.1415	−0.4059	3.45	−0.0218	−0.0143	0.172	0.105	−0.0429	0.143	0.0065
		1.0	2.180	1.090	−0.1306	5.80	−0.0019	−0.0022	0.0263	0.0157	−0.0041	0.0252	0.0015
		10	2.102	1.051	2.537	407	0.0006	0.0040	−0.0416	−0.0278	0.0041	−0.0490	−0.0032
3	9	0	2.790	1.395	0.6276	3.69	0.0089	−0.0205	−0.0776	0.177	−0.166	−0.0476	−0.0124
		0.1	2.782	1.391	0.8018	4.60	0.0091	−0.0237	−0.0878	0.204	−0.191	−0.0494	−0.0140
		1.0	2.751	1.3755	2.417	19.4	0.0067	−0.0356	−0.115	0.363	−0.278	−0.0404	−0.0188
		10	2.7276	1.3638	18.91	807	0.0013	−0.0437	−0.120	0.369	−0.332	−0.0191	−0.0211
1	10	0	1.436	0.359	−1.577	1.04	−0.298	0.116	1.325	−1.391	−1.355	−1.289	−0.228
		0.1	1.408	0.352	−1.744	1.28	−0.278	0.120	1.331	−1.438	−1.409	−1.303	−0.236
		1.0	1.2925	0.3231	−3.432	5.32	−0.156	0.136	1.234	−1.637	−1.614	−1.357	−0.271
		10	1.2055	0.3014	−21.58	222	−0.0271	0.157	1.075	−1.887	−1.866	−1.460	−0.312

[a] Load W suddenly applied at point shown in Fig. 4(*b*) and maintained constant.

[b] $\gamma_b = (a_n L_1)\, k_b d/L_1$, k_b = nozzle flexibility factor.

[c] See Appendix A for significance of these parameters.

Table 12. Nozzle flexibility factor k_b for the nozzle to act almost like a hinge

d/L_1	k_b to make $\gamma_b = 10$ for $(a_n L_1)/\pi$ of					
	0.7	1.0	1.5	2.0	2.5	3.0
0.10	45.5	31.8	21.2	15.9	12.7	10.6
0.05	90.9	63.7	42.4	31.8	25.5	21.2
0.025	182	127	84.9	63.7	50.9	42.4

Table 11 shows support loads on a mode-by-mode basis and, if all significant modes were included, the total support loads would be obtained by summing the loads for each mode. The individual mode contributions are relevant to dynamic loadings such as those resulting from earthquakes. However, for the simple dynamic loading that causes the support loads shown in Table 11, the results of static analyses with a dynamic load factor of 2.0 shown in Table 6 is more informative.

The third line of each group in Table 6 shows loads for a hinge at the nozzle essentially equivalent to $\gamma_b > 10$. Comparisons of the first and third lines in each group indicate the maximum effect of nozzle flexibility. Of course, the moment at the nozzle goes to zero for large values of γ_b. Other loads increase substantially (e.g., for $L_2/L_1 = 0.25$, F_{2y} and F_{1x} increase by a factor of 1.58). This again illustrates the point previously made that, in general, it is impossible to define a conservative flexibility factor for either static or dynamic loads.

5. SUPPORT CHARACTERISTICS

5.1 Anchors

By definition, an anchor is a support that prevents rotation or displacement in any direction. In terms of a piping system analysis, the six degrees of freedom are all set equal to zero.

Of course, no support is absolutely rigid; hence, none of the six rotations/displacements is actually zero. The discussion of nozzle flexibility in Sect. 4 indicates that if the rigidity of the anchor is such that

$$\beta < \frac{Md}{EI} , \tag{18}$$

the effect of anchor rotations will be small. In Eq. (18), β is the rotation in any direction, d and I are the diameter and moment of inertia of the pipe being anchored, and M is the moment in any direction. Having obtained adequate rotational rigidity, the displacement rigidity will probably be adequate and the lowest natural frequency of the anchor will probably be above the earthquake range (e.g., >30 Hz).

5.2 Other Restraints

By other restraints, we mean those supports that are intended to prevent motion in five or fewer degrees of freedom. For example, a guide may be used to restrict rotations and displacements in two directions. Because a guide permits motion along the axis of the pipe, it must have a clearance or gap. A pair of tie rods may be used to restrict displacement in one plus or minus direction. Because the rods are attached to pipe by bolted clamps, clearances exist between the bolts and bolt holes. A pipe supported on a roller (for weight support) will restrict displacement in one direction. Restraints that are intended to permit one or more motions often have frictional resistance to the presumed unrestricted motion.

In a static loading analysis, the effect of gaps, one-way displacement restraints, and frictional effects can be readily included in most piping systems analysis computer programs. In practice, one-way displacements are usually included in the analysis; frictional effects and gaps are seldom included.

In a dynamic analysis, the effect of gaps and frictional effects are seldom included. To evaluate these and other nonlinear effects, a time-history analysis must be used rather than the much less expensive linear-modal superposition analysis.

In addition to the nonlinear effects, the flexibility of the supports may be significant. As a simple example, hanger rods are designed so that the allowable load produces a nominal stress of 9000 psi in the thread root area. The deflection at the allowable load is then

$$\delta = (9000/E)L = 0.0003L \ , \tag{19}$$

for E = modulus of elasticity = 3×10^7 psi and L = length of hanger rod in inches.

It is relevant, mainly as a lead-in to Sect. 5.3, to compare the displacement of a hanger rod with thermal displacements as given by the equation

$$\delta_{th} = \alpha \Delta T L_p \ , \tag{20}$$

where α = coefficient of thermal expansion of the pipe material, ΔT is the piping temperature change, and L_p is the length of pipe. The relationship between δ_{th} and δ is

$$\delta_{th} = [\Delta T x L_p/(50xL)]\delta \ , \tag{21}$$

for $\alpha = 6 \times 10^{-6}$ in./in./°F. Now, as an example, let us assume that the length of pipe L_p that influences the displacement at the hanger is 20d and the length of the hanger rod is d. Then, for $\Delta T = 50°F$, $\delta_{th} = \delta$. If δ_{th} is in a direction to unload the hanger, the thermal expansion would do so and a piping system analysis that assumes a rigid hanger would be incorrect. Of course, a hanger rod has other sources of flexibility, such as the piping clamp, clevises, or turnbuckles. However, the message remains: rigid (or assumed rigid) restraints should be used with caution at points in a piping system where thermal expansion may occur in the direction of the restraint. As discussed in Sect. 5.3, spring hangers or constant-load hangers can be used.

For large displacements, another type of nonlinearity may occur that could be very significant. As an example, consider a hanger used to carry weight. The length of the hanger is equal to the pipe diameter d, and the hanger is located in a span of pipe such that, when subjected to a dynamic load, the pipe has a horizontal deflection equal to $d/\sqrt{2}$. The hanger is, therefore, at a 45° angle to the horizontal and is restraining the horizontal motion as well as the weight. Thus, the load on the hanger might be subjected to loads that are several times those anticipated from the analysis. This nonlinear effect may contribute to the explanation of failures of hangers during dynamic loads such as severe water-hammers.

In both static and dynamic analyses, the effect of support flexibility can be included in the piping system analysis with relatively little difficulty. Brussalis[19] gives results of a study that included the effects of support stiffness as well as nonlinear effects associated with snubbers (see Sect. 5.4); Barta et al.[20] shows extensive comparisons between various types of earthquake analyses (linear modal superposition, with and without support flexibility and time-history analyses with various snubber gaps). An EPRI report[21] on testing and analysis of feedwater piping at Indian Point Unit 1 includes investigations of the effect of assumed support stiffness on calculated dynamic responses of piping systems. However, we are not aware of any study of the large displacement nonlinearity discussed in the preceding paragraph.

5.3 Spring and Constant-Load Supports

Variable-load spring hangers are used to support the piping systems where there is a moderate amount of thermal expansion movement. These are available in a variety of load ratings and spring rates. Such hangers are normally furnished with a turnbuckle so that the load can be set to accommodate both the cold and hot load. The flexibility of variable-load spring hangers can be and is normally included in both static- and dynamic-piping-system analyses. If properly selected and installed, variable-load spring hangers should behave like linear elastic springs, although like hanger rods, gaps resulting from clearances between bolts and bolt holes will exist.

Constant-load spring hangers are used for support* of piping systems where there is a large amount of thermal expansion movement or where, for some other reason, a constant-load support is desirable. Constant-load spring hangers involve a mechanical linkage between the load and a spring such that, over the rated displacement, the load should remain essentially constant. The loads of constant-load hangers can be and are normally included in a static analysis. Figure 7, from page A-5 of NUREG/CR-3180,[22] shows measured force-deflection curves for some "constant-force hangers." One might speculate that such force-deflection curves would depend upon the length of time in service and service environment (e.g., corrosion of linkage pins), how frequently (if ever) lubricated, and the details of the particular manufacturer's design (e.g., linkage pin clearance). These aspects are not discussed in Blakely et al.[22] Figure 7 was presumably developed under quasi-static loading. The force-deflection response at a constant-load hanger might be quite different under dynamic loading.

Another type of constant-load support that is fairly commonly used in high-temperature industrial piping systems consists of a weight connected by a flexible cable through a pulley to the pipe. We mention this type mainly to call attention again to potential problems of appropriately modeling constant-load hangers for dynamic analysis. The support load of interest, in this case, would be the support of the pulley.

5.4 Snubbers

Snubbers are intended to permit slow movement, such as that resulting from thermal expansion of the piping, but to prevent fast movements, such as those resulting from an earthquake or a water hammer. Snubbers are usually attached to the pipe by pipe clamps and to the building structure through adjustable tie rods; they involve the flexibility and gaps of those attachments. Further, the mechanical action of snubbers is usually nonlinear for small displacements.

---

*The piping designer using constant-load supports of a piping system should be aware of the potential for large displacements due to unexpected weight loadings. Travel stops built into constant-load hangers may be the only restriction to the displacements.

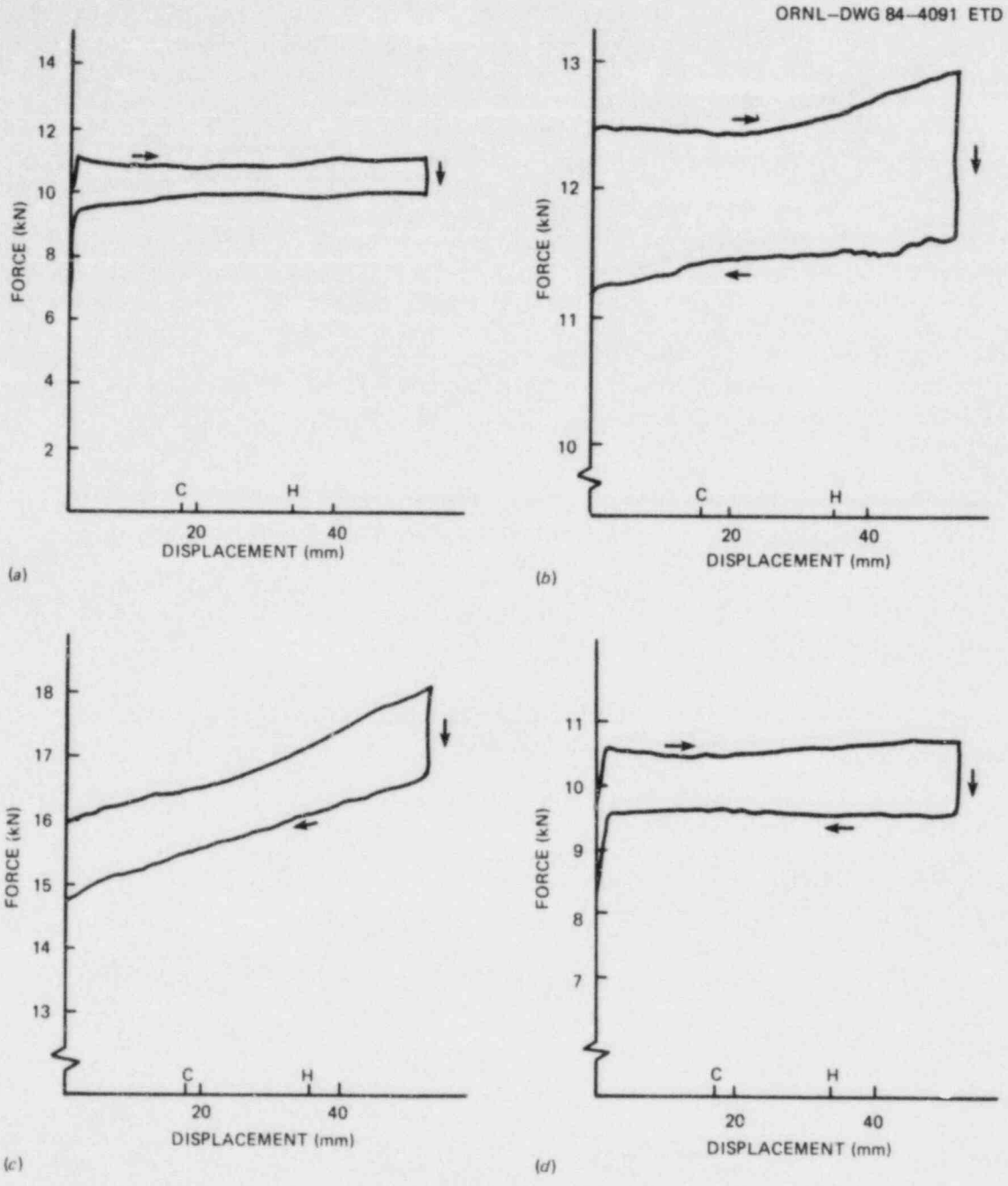

Fig. 7. Experimentally determined force-displacement characteristics of some "constant-force hangers." (*a*) Constant-force hanger 5, (*b*) constant force hanger 6, (*c*) constant-force hanger 7, and (*d*) constant-force hanger 4. Source: K. D. Blakely et al., "Pipe Damping Studies and Nonlinear Pipe Benchmarks from Snapback Tests at the Heissdampfreaktor," ANCO Engineering, Inc., NUREG/CR-3180, July 1983.

In a static analysis, snubbers are usually assumed to produce zero load. However, in small piping, the weight of the snubber and frictional resistance to slow movement may be significant. Also, snubbers may malfunction and "lock up." The snubber then becomes the equivalent of a "rigid" restraint and, because snubbers are used where thermal expansion displacement is significant,* the pipe, the snubber, and/or the attachments may be overloaded.

In a dynamic analysis, snubbers are usually assumed to provide zero displacement along the axis of the snubber. Several papers[23,24] have been published on more realistic modeling of snubbers for a dynamic analysis. These papers indicate that the actual response of snubbers to dynamic loads is nonlinear and the response, in detail, depends on such parameters as the velocity, frequency, stroke position, and magnitude of load. There may be a "dead band," resulting from the flow control actuation time. In addition, snubbers involve tie rods to the pipe and building structure and some sort of pipe clamp; hence, they have flexibilities and gaps like other linear restraints. All of these characteristics feed back into the piping system dynamic analysis, adding another uncertainty to calculated support loads.

Snubbers in nuclear power plant piping are mainly used to reduce calculated stresses in the piping or calculated loads on equipment nozzles resulting from earthquakes. As discussed in Sect. 2.3.2, earthquake analysis is deemed to be highly uncertain and the response of snubbers is probably a minor part of the total uncertainty.

---

*For dynamic restraint at points of small thermal expansion displacement, a "rigid" restraint should be used.

☆U.S. GOVERNMENT PRINTING OFFICE:1984 -746 -067/ 4037 REGION NO. 4

6. CONSTRUCTION MISALIGNMENTS

During construction of piping systems, the closing joint (weld or flange) cannot be expected to line up exactly. In most cases, forces of insignificant magnitude can be applied to obtain suitable alignment for welding or inserting the bolts in flanged joints. However, the possibility that significant forces may be used in construction to compensate for misalignments is a part of uncertainties in support loads. Because such loads are "displacement controlled," a small amount of yielding of some portion of the piping and/or its restraints usually suffices to keep these kinds of loads within acceptable bounds (see Sect. 8).

7. BUILDING STRUCTURE FLEXIBILITY

Figures 1 and 4 indicate fixed points in space by the conventional symbol of a line with some hash marks. The assumption is that whatever structure connects these points is very rigid compared to the pipe. For example, in Fig. 1, the structure connecting Node 1 to Node 12 is assumed to be very rigid compared to the rigidity of the pipe between Nodes 1 and 12. We call this connecting structure the building structure.

For small piping, there is usually little question about the assumption that the building structure is rigid relative to the piping. However, for large piping (e.g., 30-in. diam), it is not apparent that the assumption is true. For some perspective, consider a building structure between the two anchor points indicated in Fig. 4(*a*) connecting 30- by 0.375-in. wall pipe. The building structure consists of a 30-in.-deep by 15-in.-flange-width I-beam, and we want the building structure to be 4 times as rigid as the pipe. Thus, the thickness of the I-beam must be about 2.84 in. (524 lb/ft I-beam!). Of course, the flexibility of a 30- by 0.375-in. elbow would mitigate the requirement for building structure. Nevertheless, it is apparent that, for large piping, building structure rigidity also contributes to uncertainties in piping support calculated loads.

8. INELASTIC EFFECTS

As mentioned in Sect. 2.4, current routine piping system analyses are based on linear elastic theory. Studies have been made of the effect of gaps and nonlinearities, in particular, of snubbers. Section 3.3 describes a nonlinear (with regard to pressure) aspect of elbow behavior. However, these analyses are based on elastic theory. Accordingly, a significant assumption is that loads on the piping and its supports do not cause gross plastic deformation. This assumption is discussed in the following section on piping and in Sect. 8.2 on supports.

8.1 Piping

The primary-plus-secondary stress-range limit for Class 1 piping is $3S_m$. Table 13 shows values of $3S_m$, yield strength S_y, and the ratio $(3S_m/S_y)$ for representative piping materials and temperatures. The ratios $(3S_m/S_y)$ range from 1.7 to 2.7. It is thus apparent that inelastic effects can occur in Class 1 piping systems under normal operating loads.

The equivalent stress-range limit for Class 2 or 3 piping is given by the equation

$$iM/Z \leq f(1.25S_c + 0.25S_h) \ . \qquad (22)$$

Table 13 shows values of S_c and S_h and the ratio $2(1.25S_c + 0.25S_h)/S_y$. In this ratio, the value of f is implied to be 1.00, which is typical in analysis of Class 2 or 3 piping systems. The factor of 2 in the ratio reflects the fact that iM/Z, for elbows, gives about one-half of the elastic stress. The ratios of $2(1.25S_c + S_h)/S_y$ range from 1.3 to 2.9. It is thus apparent that inelastic effects can also occur in Class 2 or 3 piping systems under normal operating loads.

To illustrate the significance of inelastic effects on support loads, we continue with Example 4 of Table 3 in conjunction with

a. SA-312 Type 304 material and
b. thermal expansion for a temperature increase from 70 to 550°F; $\alpha\Delta T = (9.45 \times 10^{-6})(550 - 70) = 0.004536$.

Table 3 support loads and moment M_e at the middle of the elbow are based on $\alpha\Delta T = 0.003019$; hence, for this example the elastic-based loads and elbow moment are obtained by multiplying the Table 1 values by (0.004536/0.003019) = 1.503. The maximum calculated elastic stress occurs at the middle of the elbow and is

$$S_{max} = (1.95/h^{2/3}) \times 783{,}000 \times 1.503/255 = 49{,}800 \text{ psi} \ , \qquad (23)$$

Table 13. Representative piping material properties, allowable stresses, and ratios to material yield strength

Material	Temperature (°F)	S_m (ksi)	S_y (ksi)	S_c (ksi)	S_h (ksi)	$3S_m/S_y$	$2(S_A)_1/S_y$[a]	$2(S_A)_2/S_y$[b]
106-B	100	20.0	35.0	15.0	15.0	1.71	1.29	2.14
	550	18.1	27.1	15.0	15.0	2.00	1.66	2.77
106-C	100	23.3	40.0	17.5	17.5	1.75	1.31	2.19
	550	20.65	31.0	17.5	17.5	2.00	1.69	2.82
TP304	100	20.0	30.0	18.8	18.8	2.00	1.88	3.13
	550	16.95	18.8	18.8	15.9	2.71	2.92	4.61
TP316	100	20.0	30.0	18.8	18.8	2.00	1.88	3.13
	550	17.5	19.35	18.8	17.5	2.71	2.88	4.69

[a] $(S_A)_1 = 1.25\ S_c + 0.25\ S_h$. The factor of 2 is used because, for elbows, $i = C_2/2$.

[b] $(S_A)_2 = 1.25\ (S_c + S_h)$. This corresponds to Code Class 2 or 3 stress limit when pressure and weight stresses are negligible.

for Class 1 piping, and

$$S_{max} = (1.80/h^{2/3}) \times 783{,}000 \times 1.503/255 = 45{,}900 \text{ psi} , \quad (24)$$

for Class 2 or 3 piping. In Eqs. (23) and (24), $h = tR/r^2 = 0.0769$ and $Z = 255$ in.^{3} for the 30-in.-OD, 0.375-in.-wall, 45-in. bend radius elbow. As indicated by footnote (1) of Code Table NB-3222-1, the usual practice in determining S_m for a cycle involving different temperatures is to use the average of S_m at the cold and hot temperatures; in this example, $S_m = (20{,}000 + 16{,}950)/2$ and $3S_m = 55{,}425$ psi. The value of $2(1.25S_c + 0.25S_h)$ is $2(1.25 \times 18{,}800 + 0.25 \times 15{,}900) = 54{,}950$ psi. Accordingly, the example has calculated elastic stresses that are below Code allowables.

We now postulate that the "piping system," in Fig. 4(*a*), is heated so that the temperature increases linearly with time over a period of 8 h or more, so that the time-dependency of inelastic effects is negligible. The maximum elastic stress in the elbow can then be related to the temperature T by

$$S(T) = [(T - 70)/480] \times 49{,}800 , \quad (25)$$

where we use the elbow stress from Eq. (23) (also used in succeeding equations).

The material yield strength can be expressed as

$$S_y = 31{,}630 - 23.3T . \quad (26)$$

By equating $S(T)$ to S_y, we find that the temperature T_1 at which inelastic effects begin is obtained from:

$$[(T_1 - 70)/480] \times 49{,}800 = 31{,}630 - 23.3T_1 , \quad (27)$$

thus, $T_1 = 306°F$. However, the inelastic effects are quite small until the load produces through-the-wall plasticity. Before gross plastic deformation can occur, the yield stress level must propagate through the wall. For an elbow, the maximum stress is almost pure through-the-wall bending; hence, the loads must be increased by a factor of about 1.5 before gross plastic deformations occur. This aspect can be included in the example by dividing the calculated stresses by 1.5. Thus, dividing the left-hand side of Eq. (27) by 1.5, gives

$$T_1 = T_p = 394°F . \quad (28)$$

Accordingly, during the heat-up to 394°F, the elastic analysis is reasonably valid.

Kachanov[25] and Spence and Mackenzie[26] have developed theories that lead to an effective elbow flexibility factor k_{ep}, in the plastic region. Material properties are represented by the equation*

$$e = A\sigma^n , \tag{29}$$

where e is the plastic strain, A is a constant, σ is the stress, and n is a constant. In contrast to the elastic region, where k is closely approximated as 1.65/h, $\geq$1.0, the value of k_{ep} is dependent on the exponent n in Eq. (29) as well as the elbow parameter $h = tR/r^2$ and cannot be expressed as a simple relationship. For example, for n = 3 and h = 0.10, k_{ep} = 232 as compared with k = 16.5 (elastic solution, n = 1.0). These theories do not include end effects, which, even for long straight pipes attached to both ends, may be quite significant. For the example used here in which h = 0.0769, we use $k_{ep} = 20k = 429$. This value of k_{ep} is deemed to be reasonably representative of the Type 304 material elbow at temperatures up to 550°F.

Table 14 summarizes the elastic-plastic calculations. The first line, the initial 70°F condition, shows a row of zeros. The assumption is that stresses resulting from weight and construction misalignments are negligible. The second line, the 394°F condition, shows the elastic loads at that temperature. The maximum pipe stress divided by 1.3 (its plastic shape factor) is less than S_y; hence, gross pipe yielding is not yet involved.

The third line in Table 14, ΔT, shows the increment in loads and stresses as the temperature is increased from 394 to 550°F. These are calculated using $k = k_{ep} = 429$ and thermal expansion of $9.45 \times 10^{-6} \times (550 - 394) = 0.00147$. The fourth line, 550EP, shows the sum of the second and third lines and is the elastic-plastic solution. The pipe stress is slightly more than $1.3S_y$; hence, in principle, the solution is not accurate. The plastic response of the pipe could, of course, be included in an elastic-plastic analysis.

The fifth line shows the elastic solution. During cool-down to 70°F, these loads will be removed. In the absence of any reverse yielding, the loads at the return to 70°F are given by the elastic-plastic solution minus the elastic solution. These values are shown in the last line of Table 14. Because the stresses divided by the plastic shape factors at return to 70°F are less than S_y, reverse yielding does not occur in this example. If, after this heat-up cool-down cycle, the pipe were cut at Point 2 of Fig. 4(*a*), for example, the pipe would move in response to the reduction of F_x, F_y, and M_2 to zero. This phenomenon has been observed in the field and sometimes is erroneously taken to be evidence of construction misalignments.

Figure 8(*a*) illustrates the variation of effective elbow stress with temperature. As indicated by the arrows, subsequent heat-up cool-down cycles give a linear relationship. Figure 8(*b*) is a conceptual representation of a condition of reverse yielding. To illustrate the concept,

---

*Although the theory in Spence and Mackenzie[26] is for stationary creep, it is applicable to time-independent plasticity by replacing strain rate with plastic strain.

Table 14. Example[a] of inelastic effects on support loads

Temperature[b] (°F)	F_x (lb)	F_y (lb)	M_2 (in.-kip)	M_1 (in.-kip)	M_e (in.-kip)	$\frac{M_2/Z}{1.3}$ (ksi)	$\frac{C_2Me/Z}{1.5}$[c] (ksi)	S_y (ksi)
70	0	0	0	0	0	0	0	30.0
394	19,200	−19,200	−4440	−4440	794	13.4	22.4	22.4
ΔT	7,000	−7,000	−1850	−1850	61			
550EP	26,200	−26,200	−6290	−6290	855	19.0	24.1	18.8
550E	28,400	−28,400	−6580	−6580	1180			
70	−2,200	2,200	290	290	−325	6.64	9.16	30.0

[a]Example No. 4 in Table 3, for TP.304 material, $\alpha\Delta T = 0.004536$ instead of $\alpha\Delta T = 0.003019$ in Table 3.

[b]Second 70 is for return to 70°F. ΔT = (550−394)°F, during which temperature increase the elbow undergoes plastic deformation. The elbow plastic theory includes strain hardening, hence $(C_2M_e/Z)/1.5$ is greater than S_y at 550°F.

[c]$C_2 = 1.95/h^{2/3} = 1.95/0.0769^{2/3} = 10.783$.

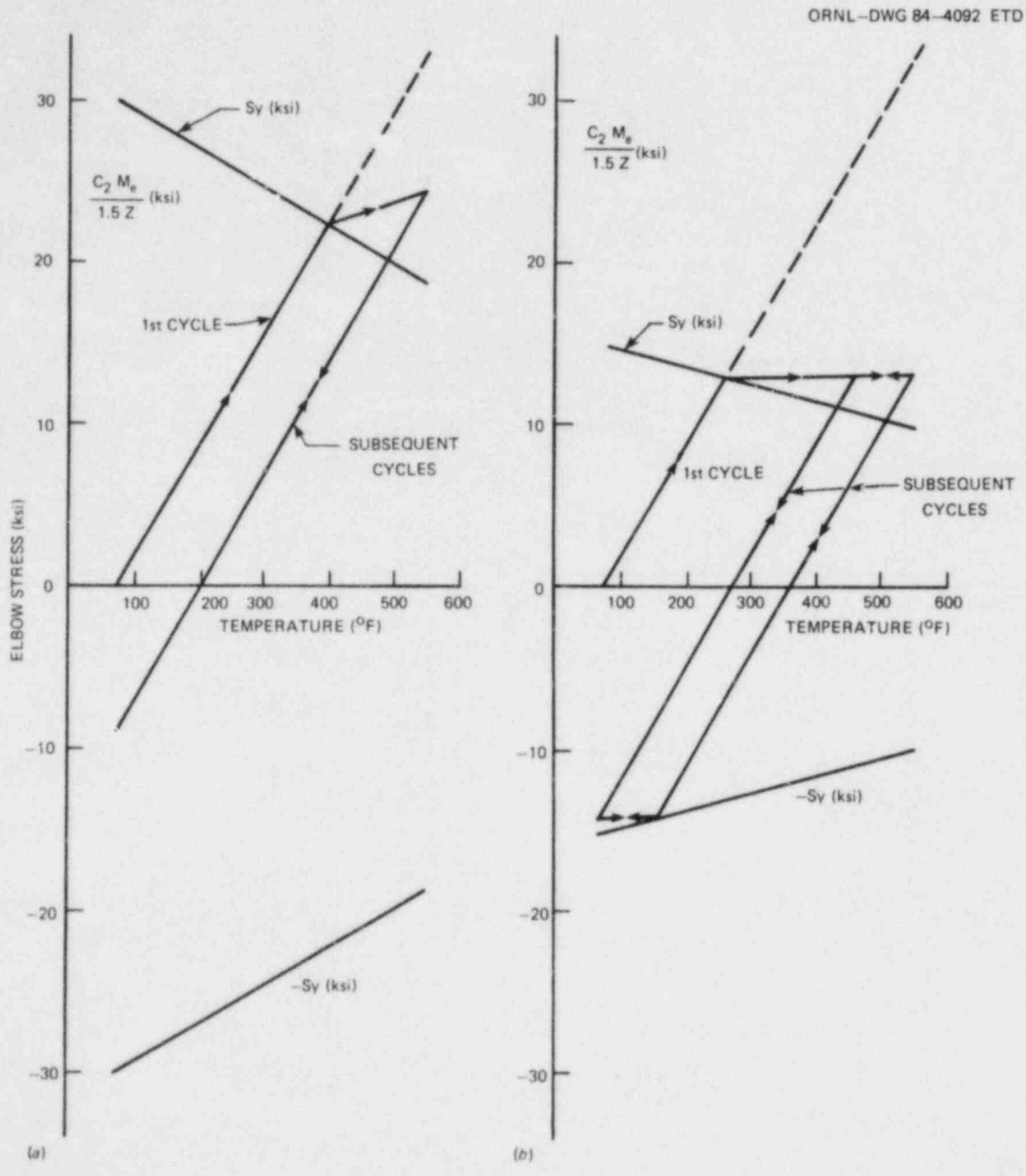

Fig. 8. Illustration of elastic-plastic elbow characteristics. (*a*) Text example and (*b*) conceptual example with reverse yielding.

the material yield strength is assumed to be one-half of that given by Eq. (26) and k_{ep} is assumed to be very large. After the first cycle, the elbow undergoes cyclic plasticity, assuming the material neither hardens nor softens under cyclic loading.

It can be seen in Table 14 (compare the 550E line with the 550EP line) that, in this particular example, the uncertainty in support loads resulting from inelastic effects is small. Further, noting that Eq. (25) is based on minimum specified or expected yield strengths, the actual material yield might be sufficiently higher that the elastic solution would still be correct.

A bound of support load uncertainty can be obtained by observing that both $3S_m$ and $2(1.25S_c + 0.25S_h)$ can be above $2S_y$. Accordingly, reverse yielding can occur, in which case the support loads could be overestimated by a factor of about 2. Although the support loads, in the configuration of Fig. 4(*a*), would be lower than calculated by an elastic analysis, the supports should be designed for both plus and minus loads, an aspect not apparent from an elastic analysis.

Evaluation of inelastic effects for *static* loads, including weight and anchor movements, is relatively simple, provided the yielding components consist of straight pipe or elbows. The inelastic response of branch connections, tees, and nozzles, however, has not been adequately developed.

Evaluation of inelastic effects for *dynamic* loads is much more complex. Inelastic effects would change the frequency of the piping system and probably increase the damping significantly. Also, time-dependency of plastic flow might become significant, even for the relatively slow earthquake responses.

8.2 Supports

Piping supports are covered by Subsection NF of the Code. For Level A (normal operating conditions) primary membrane stresses are limited to S_m for Class 1 or S for Class 2 or 3 supports. Primary membrane-plus-bending stresses are limited to $1.5S_m$ for Class 1 or 1.5S for Class 2 or 3 supports.

Piping supports are usually made of a structural carbon steel material such as SA36; the properties for SA36 are shown in Table 15.

Table 15. Properties of SA36 structural carbon steel

Temperature (°F)	S_m	S	S_y	$\frac{1.5S_m}{S_y}$	$\frac{1.5S}{S_y}$
100	19.3	14.5	36.0	0.80	0.60
550	18.5	14.5	27.85	1.00	0.78

Because the allowable stresses do not exceed S_y, gross plastic deformation of supports should not occur under normal operating conditions. It is important to note that stresses induced by restraint of thermal expansion and anchor movements of the piping are considered to be primary stresses for piping supports.

The Level B stress limits are 1.33 times the Level A limits. The primary membrane stress limits for SA36 material are below S_y, but the primary membrane-plus-bending stresses can exceed S_y. For a support consisting of an I-beam (plastic shape factor of ~1.0), this could permit gross plastic deformations in bending.

The Level C stress limits are 1.5 times the Level A limits. The Level D limits for SA36 material are about 2.0 times the Level A limits. After occurrence of a Level C or D event, the plant is intended to be shut down and examined for damage and that damage repaired, if appropriate, before resuming operation. However, because gross plastic deformation of piping supports may occur during Level C or Level D occurrences, this adds one more uncertainty to calculated support loads during such events.

9. SUMMARY AND RECOMMENDATIONS

9.1 Summary

Table 16 summarizes the sources of uncertainties discussed in this report.* The last column of Table 16 indicates the typical relative significance of the uncertainties, in the writer's judgment. As indicated, at least to some extent, by the simple examples included in the report, the uncertainties of calculated support loads are highly dependent upon the specifics of the piping system and the supports. Accordingly, the word "typical" in the judgmental evaluation should not be overlooked.

The static loading examples in Tables 3 and 10 all indicate that increasing the flexibility of piping systems leads to a decrease in support loads. However, it is pointed out that this may not be generally true. As noted in Sects. 3 and 4, this leads to the conclusion that it is impossible to define a "conservative" flexibility factor (i.e., a flexibility factor which will ensure that support loads are not underestimated in any part of the piping system). By extension, this dilemma is also applicable to inaccurate assessment of flexibility from any source (e.g., hanger or building flexibility or gaps in supports).

The list of uncertainties in Table 16 is rather lengthy and might be taken as implying that calculated support loads are likely to be significantly in error. However, for most typical piping systems, the uncertainties tend to be small and, to some extent, compensate for each other. For example, overestimating the elbow flexibilities may partially compensate for underestimating nozzle flexibilities. Further, piping systems and supports in nuclear power plants are made of ductile materials so that overloaded supports can "give" and shift excess load to redundant supports. The inelastic effects discussed in Sect. 8 are highly significant in preventing failures of supports.

9.2 Recommendations

Currently, the PVRC Steering Committee on Piping Systems (S. H. Bush, chairman) is conducting an extensive program to review the current basis for design of piping systems under dynamic loadings with the major emphasis an seismic loadings. The major technical areas are

1. spectral broadening,
2. seismic damping,
3. dynamic allowable stresses, and
4. industry practice.

---

*As pointed out in Sect. 1, this report does not discuss design or construction errors.

Table 16. Summary of sources of uncertainty in the calculation of loads on supports of piping systems

Section[a]	Source of uncertainty	Significance[b]
2.2	Use of nominal pipe properties: D, t, I, and weights	S
2.3.1	Weights of fluid, insulation, valves, etc.	S
2.3.1	Values of α and Δt	S
2.3.2	Earthquake dynamic loading	
	Input	L
	Analysis method	L
	Damping	L
2.3.2	Other dynamic loadings	
	Input	M
	Analysis method	M
	Damping	L
3.0	Elbow flexibility	
3.2	Nominal versus actual dimensions	M
3.3	Internal pressure effect	S
3.4	End effects	M
4.0	Nozzle flexibility	
	Nozzles to large D/T vessels or run pipe	L
	Nozzles to small D/T vessels or run pipe	S
5.0	Support characteristics	
	Flexibilities	S
	Gaps, nonlinearities (static loads)	S
	Gaps, nonlinearities (dynamic loads)	U
	Constant load support, response to dynamic loads	U
	Snubber lockup	L
6.0	Construction misalignments	S
7.0	Building structure flexibility	S
8.0	Inelastic effects	
	Static loads	M
	Dynamic loads	U

[a]Section of report in which the uncertainty is discussed.

[b]Judgmental evaluation of the typical relative significance of the uncertainty: S = small, M = medium, L = large, and U = uncertain.

The PVRC Subcommittee on Dynamic Analysis of Pressure Components is undertaking work in the following technical areas:

1. pressure transients,
2. seismic analysis,
3. missile impact, and
4. dynamic stress criteria.

The PVRC Subcommittee on Piping, Pumps, and Valves is undertaking work on allowable loads on pump nozzles.

The Electric Power Research Institute (EPRI) has conducted tests on the Indian Point Unit 1 feed-water piping and is conducting laboratory tests on straight-pipe, Z-bends, and more complex piping systems; some of the results are now available and have been compared with calculated responses.[21,27,28]

NRC-RES has undertaken a cooperative effort with the Federal Republic of Germany in the Heissdampfreaktor (HDR) testing program to study the response of piping systems subjected to various exitations. Correlations of test data with calculated responses are contained in several documents.[22,29-31]

The activities and reports mentioned above are relevant, in various degrees, to the subject of uncertainties in calculated loads on piping supports. Some of the programs may lead to reducing the conservatisms in current piping design practice (e.g., increased damping and perhaps increased dynamic allowable stresses), making use of the ability of piping to absorb plastic strains. If this occurs, it will become more important to bound the uncertainties on calculated piping support loads.

The following recommendations are made in light of the above ongoing work, with the objective of supplementing but not duplicating that ongoing work. It may be noted that the first two recommendations can be related to static as well as dynamic loadings. With the potential reductions in conservatism for dynamic load, the uncertainties in static loadings may become even more significant.

1. A sensitivity study should be made to establish the parameters (e.g., ratio of straight-pipe lengths to elbow lengths) where elbow flexibility is significant with respect to support loads. The results given in Tables 3, 4, and 5 represent an initial step toward this objective. Extension to multiplane piping systems should be included.
2. A sensitivity study should be made to establish the parameter (e.g., ratio of nozzle flexibility factor to length of piping), where nozzle flexibility is significant with respect to support loads. The results given in Tables 10 and 11 represent an initial step toward this objective. Extension to multiplane piping systems should be included.

   In addition, because limits on allowable loads on nozzles frequently control the design of piping systems (e.g., require additional supports to keep nozzle loads within bounds), the study should include development of rational, though not excessively conservative, criteria for establishing allowable loads on nozzles in pressure vessels, tanks, piping, etc.

3. Available Dynamic Loading Data Evaluation

   a. Available test data on dynamic loading of piping systems and subsystems (e.g., test on straight pipe lengths) should be searched for and accumulated.
   b. Available reports and papers that compare dynamic loading test data on piping systems with calculated responses should be searched for and accumulated. Examples of such reports are available.[21,22,27-31]
   c. An interpretive report should be prepared that addresses the questions

      i. How do calculated support loads compare with measured support loads?
      ii. How do calculated piping stresses compare with measured stresses?
      iii. If "failure" occured in a test (e.g., a crack or excessive distortion), how do the test conditions compare with allowable loadings under current piping design practice?

References 21, 22, and 27–31 concentrate almost exclusively on calculated vs measured comparisons of mode frequencies, acceleration time-histories, and displacement time histories. These are significant parameters in checking whether a given analysis method (computer program) is valid. However, current design practice entails an evaluation of load-histories on supports and stress (or pseudo-stress, for stresses above yield strength) histories in piping pressure boundaries. The cited references give relatively little data on these basic parameters from a design standpoint. However, it is believed that test data and analyses relevant to these basic parameters may be available from the authors of the cited references.

Recommendation 3 is broader than just support loads. The motivation is that having accumulated available dynamic loading data, most of the background information would be available for evaluating different dynamic stress criteria as applied to piping pressure boundaries.

REFERENCES

1. *ASME Boiler and Pressure Vessel Code, Sect. III, Nuclear Power Plant Components*, Div. 1, 1980 ed. with addendas through winter 1982, American Society of Mechanical Engineers, 345 E. 47th St., New York.

2. J. Spence and G. E. Findlay, "The Effect of Thickness Variations on the Behavior of Smooth Curved Pipe Bends Under External Bending," ASME Paper No. 78-PV9-9P, American Society of Mechanical Engineers, New York, 1978.

3. R. A. Clark, T. E. Gilroy, and E. Reissner, "Stresses and Deformations of Toroidal Shells of Elliptical Cross Section," *J. Appl. Mech.* 19, 37–48 (1952).

4. G. E. Findlay and J. Spence, "Bending of Pipe Bends with Elliptic Cross Sections," *Weld. Res. Counc. Bull.* No. 164 (August 1971).

5. E. C. Rodabaugh and H. H. George, "Effect of Internal Pressure on Flexibility and Stress-Intensification Factors of Curved Pipe or Welding Elbows," *Trans. ASME* 79, 939–48 (1957).

6. E. C. Rodabaugh and S. E. Moore, "End Effects on Elbows Subjected to Moment Loadings," ORNL/Sub-2913/7, Union Carbide Corp. Nuclear Div., Oak Ridge Natl. Lab., March 1978.

7. T. E. Pardue and J. Vigness, "Properties of Thin-Walled Curved Tubes of Short Bend Radius," *Trans. ASME* 73, 77–84 (1951).

8. J. F. Whatham, "In-Plane Bending of Flanged Pipe Elbows," *Trans. Inst. Eng.* 21(2), 80 (1979).

9. G. Thomson, and J. Spence, "The Influence of Flanged End Constraints on Smooth Curved Tubes Under In-Plane Bending," *Int. J. Press. Vessels Piping* 13(2), 65–83 (1983).

10. E. C. Rodabaugh and S. E. Moore, *Stress Indices and Flexibility Factors for Nozzles in Pressure Vessels and Piping*, NUREG/CR-0778, Union Carbide Corp. Nuclear Div., Oak Ridge Natl. Lab., June 1979.

11. C. R. Steele, *Evaluation of Reinforced Openings in Large Steel Pressure Vessels*, Shelltech Report 80-2, Shelltech Assoc., Stanford, Calif., Dec. 20, 1980.

12. L. R. Jackson et al., *Stresses in Unreinforced Branch Connections*, Battelle-Columbus Labs., Columbus, Ohio, Sept. 30, 1953.

13. E. T. Cranch, "An Experimental Investigation of Stresses in the Neighborhood of Attachments to a Cylindrical Shell," *Weld. Res. Counc. Bull.* No. 60, May 1960.

14. F. J. Mehringer and W. E. Cooper, "Experimental Determinations of Stresses in the Vicinity of Pipe Appendages to a Cylindrical Shell," p. 159 in *Proc. Soc. Exp. Stress Analy.* 14(2), 1957.

15. Chicago Bridge and Iron Company, *Experimental Testing Program for Nozzle Connections in Cylindrical Shells*, CBI Report No. 74-9453, Chicago, Ill., 1979.

16. H. Dykstra and R. A. Whipple, *Cylindrical Shell Stresses Due to Penetration Loads where R/T = 1200*, CBI Report R-0242-1, April 1980.

17. R. A. Whipple, J. Hagstrom, and H. Dykstra, "Experimental Investigation of Cylindrical Shell Stresses due to Penetration Loads Where R/T = 1264," *ASME J. Pressure Vessel Technol.* 105, 201–206 (August 1983).

18. J. Schroeder, *Experimental Validation of the Evaluation of Reinforced Openings in Large Steel Pressure Vessels*, Final Report to PVRC Subcommittee on Reinforced Openings and External Loadings, Univ. of Waterloo, Waterloo, Canada, January 1983.

19. W. G. Brussalis, "Comparison of Linear and Nonlinear Seismic Analysis of Piping," pp. 27–39 in *Effects of Piping Restraints on Piping Integrity*, ASME Publication PVP-40, American Society of Mechanical Engineers, New York, 1980.

20. D. A. Barta, S. N. Huang, and L. K. Severud, "Seismic Analysis of Piping with Nonlinear Supports," pp. 439–48 in *Pressure Vessels and Piping: Design Technology-1982 – A Decade of Progress*, ASME Book No. G00213, American Society of Mechanical Engineers, New York, 1982.

21. *Testing and Analysis of Feedwater Piping at Indian Point Unit 1, Volume 1, Damping and Frequency*, EPRI NP-3108, Electric Power Research Institute, Palo Alto, Calif., July 1983.

22. K. D. Blakely et al., *Pipe Damping Studies and Nonlinear Pipe Benchmarks from Snapback Tests at the Heissdampfreaktor*, NUREG/CR-3180, ANCO Engineers, Inc., Culver City, Calif., July 1983.

23. M. C. Pickett and J. R. Gartner, "Development of a Nonlinear Frequency and Load Dependent Model for Velocity Sensitive Hydraulic Snubbers," pp. 81–93 of *Recent Advances in Pipe Support Design*, ASME Publication PVP-68, American Society of Mechanical Engineers, New York, 1982.

24. B. J. Cheek, R. A. Meyer, and E. O. Swain, eds., *Criteria for Nuclear Safety Related Piping and Component Support Snubbers*, ASME Publication PVP-45, American Society of Mechanical Engineers, New York, 1980.

25. L. M. Kachanov, "Plastic Bending of Curved Tubes," *Izv. Akad. Nauk. SSSR Otd. Tekh. Nauk* 5 (1957).

26. J. Spence and A. C. Mackenzie, "Stationary Creep Deformation of a Smooth Pipe Bend Under In-Plane Bending Moments," *Int. J. Mech. Sci.* 11, 387–94 (1969).

27. D. K. Morton, J. R. Olsen, and R. G. Rahl, "Prediction and Comparison of Z-bend Responses when Subjected to Simulated Seismic Loads," EGG-EA-6368, Idaho Natl. Engineering Lab., Idaho Falls, Idaho, August 1983.

28. P. Bezler, M. Subudhi, and S. Shteyngart, *In Situ and Laboratory Benchmarking of Computer Codes Used in Dynamic Response Predictions of Nuclear Reactor Piping*, NUREG/CR-3340, Brookhaven Natl. Lab., Long Island, N.Y., May 1983.

29. D. P. Finicle, R. C. Guenzler, and R. G. Rahl, *HDR Response — Experimental and Analytical*, NUREG/CR-1913, EG&G Idaho, Inc., Idaho Falls, Idaho, February 1981.

30. W. B. Walton, G. H. Howard, and B. Johnson, *German Standard Problem 4a*, NUREG/CR-2390, ANCO Engineers, Inc., Culver City, Calif., November 1981.

31. G. L. Thinnes and R. G. Rahl, *Experimental and Analytical Results of Blast Induced Seismic Studies at HDR*, NUREG/CR-2463, Idaho National Engineering Lab., Idaho Falls, Idaho, November 1981.

Appendix A

DYNAMIC LOADING THEORY

Rather than use one of the many existing computer programs for dynamic analysis of piping, it was expedient to develop the theory for the simple configuration and loading that was used as an example in this report. The parameters of interest (elbow and nozzle flexibilities) could then be varied quickly and inexpensively.

A.1 Theory

The theory for structures with distributed mass and load given by Biggs[A1] is used as the basis of the development. The model is shown in Fig. 4(*b*) and (*c*).

A.1.1 Leg 1

The modal shape of Leg 1 is given* by

$$\Phi(x_1) = A_1 \sin a_n x_1 + A_2 \cos a_n x_1 + A_5 \sinh a_n x_1 + A_6 \cosh a_n x_1 , \qquad (A.1)$$

where

$A_1 \ldots A_6$ are constants of integration,

$a_n = (m w_n^2/EI)^{1/4}$, (A.2)

m = mass per unit length of pipe,

w_n = natural frequency of n-th mode,

E = modulus of elasticity of pipe material,

I = moment of inertia of pipe cross section.

As detailed in the following, three of the four constants and a_n can be determined from boundary conditions at the ends of Leg 1. The other constant (which we selected to be A_2) can then be determined for a specific type of dynamic loading.

For Leg 1, the boundary condition $y_1 = 0$ at $x_1 = 0$ gives $A_1 = -A_6$; hence, Eq. (A.1) is reduced to

$$\Phi(x_1) = A_1 S + A_2(C - CH) + A_5 SH , \qquad (A.3)$$

where $S = \sin a_n x_1$, $C = \cos a_n x_1$, $CH = \cosh a_n x_1$, and $SH = \sinh a_n x_1$.

---

*See Eq. 4.5 of Ref. A1.

For Leg 1, the boundary at $x_1 = 0$ involves the nozzle flexibility, which is represented by a point spring at location 1 [see Fig. 4(*b*)]. This, of course, is consistent with the Code definition of a nozzle flexibility factor. The moment-rotation relationship is

$$M_1 = [EI/(k_b d)]\phi \ , \tag{A.4}$$

where the subscript b has been added to distinguish the nozzle flexibility factor from the elbow flexibility factor k. Equation (A.4) leads to the boundary condition

$$-EIy_1'' = -EIy_1'/(k_b d) \text{ at } x_1 = 0 \ , \tag{A.5}$$

and, by differentiating Eq. (A.3),

$$[-A_1 S_0 + A_2(-C_0 - CH_0) + A_5 SH_0]\, a_n^2 = [A_1 C_0 + A_2(-S_0 - SH_0) + A_5\, CH_0]a_n/k_b d \ , \tag{A.6}$$

where $S_0 = \sin 0$, etc. Equation (A.6) gives

$$-2A_2 a_n^2 = (A_1 + A_5)a_n/k_b d \ , \tag{A.7}$$

or

$$A_5 = -2\gamma_b A_2 - A_1 \ , \tag{A.8}$$

where

$$\gamma_b = a_n k_b d \ . \tag{A.9}$$

Equation (A.3) for Leg 1 can then be written as

$$\Phi(x_1) = A_1(S - SH) + A_2(C - CH - 2\gamma_b SH) \ . \tag{A.10}$$

From the boundary condition $y_1 = 0$ at $x_1 = L_1$,

$$A_1/A_2 = -(C_1 - CH_1 - 2\gamma_b SH_1)/(S_1 - SH_1) \ , \tag{A.11}$$

where $C_1 = \cos a_n L_1$, etc. Equation (A.10) for Leg 1 can then be written as

$$\Phi(x_1) = A_2\,[(A_1/A_2)\,(S - SH) + C - CH - 2\gamma_b\, SH] \ , \tag{A.12}$$

and the derivatives are

$$\Phi'(x_1) = A_2[(A_1/A_2)\ (C - CH) - S - SH - 2\gamma_b\ CH]a_n\ , \tag{A.13}$$

$$\Phi''(x_1) = A_2[(A_1/A_2)\ (-S - SH) - C - CH - 2\gamma_b\ SH]a_n^2\ , \tag{A.14}$$

$$\Phi'''(x_1) = A_2[(A_1/A_2)\ (-C - CH) + S - SH - 2\gamma_b\ CH]a_n^3\ . \tag{A.15}$$

A.1.2 Leg 2

Equation (A.1), with a different set of constants, also applies to Leg 2. However, from the boundary condition $y_2 = 0$ at $x_2 = 0$ and $y_2' = 0$ at $x_2 = 0$, we immediately obtain

$$\Phi(x_2) = A_3(S - SH) + A_4(C - CH)\ , \tag{A.16}$$

where $S = \sin a_n L_2$, etc., and A_3 and A_4 are constants of integration. The boundary condition $y_2 = 0$ at $x_2 = L_2$ gives

$$A_3/A_4 = -(C_2 - CH_2)/(S_2 - SH_2)\ , \tag{A.17}$$

where $C_2 = \cos a_n L_2$, etc. Equation (A.16) can then be written as

$$\Phi(x_2) = A_4[(A_3/A_4)\ (S - SH) + C - CH]\ , \tag{A.18}$$

and the derivatives are

$$\Phi'(x_2) = A_4[(A_3/A_4)\ (C - CH) - S - SH]a_n\ , \tag{A.19}$$

$$\Phi''(x_2) = A_4[(A_3/A_4)\ (-S - SH) - C - CH]a_n^2\ , \tag{A.20}$$

$$\Phi'''(x_2) = A_4[(A_3/A_4)\ (-C - CH) + S - SH]a_n^3\ . \tag{A.21}$$

A.1.3 Juncture of Leg 1 and 2

The boundary at the juncture involves the elbow flexibility factor. The elbow is represented by a point spring at J. This was done to simplify the analysis but means that the analysis is valid only if L_1/R and L_2/R are greater than about 10. The moment-rotation relationship, for the 90° elbow involved in the model, is

$$M_J = [2EI/(\pi kR)]\theta\ , \tag{A.22}$$

where k is the elbow flexibility factor. Noting that $\Phi = y_1' + y_2'$, Eq. (A.22) gives

$$-EIy_1'' = [2\ EI/(\pi kR)]\ (y_1' + y_2') \text{ at } x_1 = L_1,\ x_2 = L_2\ , \qquad (A.23)$$

and, from Eqs. (A.12) and (A.18) and their derivatives

$$A_2\ \{\gamma[(A_1/A_2)\ (-S_1 - SH_1) - C_1 - CH_1 - 2\gamma_b SH_1]$$
$$+ (A_1/A_2)\ (C_1 - CH_1) - S_1 - SH_1 - 2\gamma_b CH_1\}$$
$$+ A_4\ \{(A_3/A_4)\ (C_2 - CH_2) - S_2 - SH_2\} = 0\ , \qquad (A.24)$$

where

$$\gamma = \pi a_n kR/2\ . \qquad (A.25)$$

In addition, at the juncture, $M_{j1} = M_{j2}$, giving

$$A_2\ \{(A_1/A_2)\ (-S_1 - SH_1) - C_1 - CH_1 - 2\gamma_b SH_1\}$$
$$- A_4\ \{(A_3/A_4)\ (-S_2 - SH_2) - C_2 - CH_2\} = 0\ . \qquad (A.26)$$

A.1.4 Solution for modal frequencies and A_2/A_4

Equations (A.24) and (A.26) may be written as

$$b_{11}A_2 + b_{12}A_4 = 0\ , \qquad (A.27)$$

$$b_{21}A_2 - b_{22}A_4 = 0\ , \qquad (A.28)$$

where b_{11}, b_{12}, b_{21}, and b_{22} are the coefficients in braces in Eqs. (A.24) and (A.26). Then

$$b_{11}b_{22} + b_{21}b_{12} = 0\ . \qquad (A.29)$$

Combinations of a_nL_1 and a_nL_2 can be selected by iteration such that Eq. (A.29) is satisfied. The values of a_nL_1 give the modal frequency

$$w_n = [(EI/m)^{1/2}/L_1^2]\ (a_nL_1)^2\ . \qquad (A.30)$$

Also, having obtained values of a_nL_1 and a_nL_2 that satisfy Eq. (A.29), the ratio A_2/A_4 is given by

$$A_2/A_4 = -b_{12}/b_{11} = b_{22}/b_{21} \ . \tag{A.31}$$

Now, the modal shapes can be written in terms of the remaining unknown constant A_2 as

$$\Phi(x_1) = A_2[(A_1/A_2)\ (S - SH) + C - CH - 2\gamma_b SH] \ , \tag{A.32}$$

$$\Phi(x_2) = A_2(A_4/A_2)\ [(A_3/A_4)\ (S - SH) + C - CH] \ . \tag{A.33}$$

It may be noted that γ_b and γ are functions of a_n. However, it is convenient to consider them as constants. For a given value of γ or γ_b and with a_n established, k_b or k can be determined from Eq. (A.9) or (A.25).

The value of A_2, as discussed in Sect. A.1.5, depends upon the specific kind of dynamic loading. However, the modal frequencies are independent of A_2. The theory, up to this point, can provide pertinent information on how the modal frequencies vary with nozzle and elbow flexibilities.

A.1.5 Specific dynamic-loading example

The value of A_2 will depend upon the specific type of dynamic loading. For example, an earthquake may be considered to apply accelerations to the support points of the piping. Because the accelerations are a function of frequency, earthquake analysis is relatively complicated. The preceding theory, using modal participation factors, could be used. However, we here consider a simpler loading that, at least crudely, might represent a safety valve discharge loading on a piping system.

The specific loading consists of a sudden application of a force W at the point shown in Fig. 4(*b*). The force, after sudden application, is considered to remain constant. The modal response is given* by

$$y_n(x,t) = \left\{ \frac{[(A_1/A_2)\ (S_f - SH_f) + C_f - CH_f - 2\gamma_b SH_f]W}{w_n^2 m \int q^2(x)dx} \right. \times (1 - \cos w_n t) \left. \right\} q(x) \ , \tag{A.34}$$

where $S_f = \sin a_nL_1/2$, etc., and $q(x) = \Phi(x)/A_2$.

*See Eq. 4.24 of Ref. A1.

The term $(1 - \cos w_n t)$, where t = time, has a maximum* value of 2. To find maximum support loads, we use $(1 - \cos w_n t) = 2$.

The integral in Eq. (A.34) must be evaluated over both Leg 1 and Leg 2; that is,

$$\int \eta^2(x)dx = \int_o^{L_1} q_1^2(x_1)dx_1 + \int_o^{L_2} q_2^2(x_2)dx_2 \ . \qquad (A.35)$$

Noting that $q_1(x_1) = \Phi(x_1)/A_2$ and $q_2(x_2) = \Phi(x_2)/A_2$ and looking at Eqs. (A.32) and (A.33) and the squares of these expressions, it is apparent that a closed-form solution to the integrals would be difficult to derive. Accordingly, we used numerical integration to obtain the integral of Eq. (A.35).

It may be noted that the quantity in braces in Eq. (A.34) is A_2 for the particular type of dynamic loading consisting of sudden application and maintenance of a force W at the point $x_1 = L_1/2$.

A.1.6 Calculation of support loads and moments at J

The moments and forces are obtained from the general relationships

$$M = -EIy'' \ , \qquad (A.36)$$

$$F = -EIy''' \ . \qquad (A.37)$$

Support loads are identified in Fig. 4(*c*) as M_1, M_2, F_{1x}, F_{2x}, F_{1y}, and F_{2y}. The moment at the "elbow," point J in Fig. 4(*b*), is also of interest.

Equations (A.32) and (A.33) and the derivatives thereof, along with A_2 defined by the quantity in braces in Eq. (A.34), give the following equation for moments in Leg 1:

$$-M/WL_1 = 2[q(x)]_f/[Q(a_n L_1)^2] \times [(A_1/A_2)\ (-S - SH) - C - CH - 2\gamma_b SH] \ , \qquad (A.38)$$

where

$$[q(x)]_f = (A_1/A_2)\ (S_f - SH_f) + C_f - CH_f - 2\gamma_b SH_f \ , \qquad (A.39)$$

$$Q = \left[\int_o^{L_1} q_1^2(x_1)dx_1 + \int_o^{L_2} q_2^2(x_2)dx_2\right] \Big/ L_1 \ . \qquad (A.40)$$

In deriving Eq. (A.38), the relationship $w_n^2 = (EI/m)\ (a_n L_1)^4/L_1^4$ was used. This eliminates EI and m from Eq. (A.38).

---

*Damping is assumed to be negligible in the time to reach the first value of $(1 - \cos w_n t) = 2$.

For Leg 2,

$$-M/WL_1 = 2[q(x)]_f/[Q(a_nL_1)^2] \times [(A_3/A_4)\,(-S - SH) - C - CH]\,(A_4/A_2)\,. \qquad (A.41)$$

The shear forces are given for Leg 1 by

$$-F/W = 2[q(x)_f/Q(a_nL_1)] \times [(A_1/A_2)\,(-C - CH) + S - SH - 2\gamma_b CH]\,, \qquad (A.42)$$

and for Leg 2 by

$$-F/W = 2[q(x)]_f/[Q(a_nL_1)] \times [(A_3/A_4)\,(-C - CH) + S - SH]\,(A_4/A_2)\,. \qquad (A.43)$$

Reference

A1. John M. Biggs, *Introduction to Structural Dynamics*, McGraw-Hill Book Co., New York, 1964.

Appendix B

STATIC LOADING THEORY

The theory for the model shown in Fig. 4(*a*) consists of an elementary application of beam theory. Thermal expansion produces displacements δ_x and δ_y of point 2 with respect to point 1 but no rotation. The three forces are obtained from the set of equations

$$A_{11}F_x + A_{12}F_y + A_{13}M_2 = EI\delta_x \ , \tag{B.1}$$

$$A_{21}F_x + A_{22}F_y + A_{23}M_2 = -EI\delta_y \ , \tag{B.2}$$

$$A_{31}F_x + A_{32}F_y + A_{33}M_2 = 0 \ , \tag{B.3}$$

where

$$A_{11} = (L_y + R)^2 L_x + kR[(\pi/2) L_y^2 + 2L_yR + (\pi/4)R^2] + L_y^3/3 + k_s(L_y + R)^2 \ ,$$

$$A_{12} = R(L_y + R) L_x + (L_y + R) L_x^2/2 + kR^2 [(\pi/2 - 1) L_y + R/2] + k_s (L_x + R) (L_y + R) \ ,$$

$$A_{13} = (L_y + R) L_x + kR [(\pi/2) L_y + R] + L_y^2/2 + k_s (L_y + R) \ ,$$

$$A_{22} = R^2L_x + RL_x^2 + kR^3 (3\pi/4 - 2) + L_x^3/3 + k_\varepsilon (L_x + R)^2 \ ,$$

$$A_{23} = RL_x + kR^2 (\pi/2 - 1) + L_x^2/2 + k_s (L_x + R) \ ,$$

$$A_{33} = L_x + kR\pi/2 + L_y + k_s \ ,$$

$$A_{21} = A_{12}, \ A_{31} = A_{13}, \text{ and } A_{32} = A_{23} \ .$$

In the above, $L_x = (L_1 - R)$; $L_y = (L_2 - R)$; k = elbow flexibility; and $k_s = k_b/d$, the nozzle flexibility as defined by Eq. (12) divided by the pipe diameter d.

Solution of the set of equations (B.1), (B.2), and (B.3) gives F_x, F_y, and M_2. The moment M_1 [see Fig. 4(*a*)] is

$$M_1 = F_xL_2 + F_yL_1 + M_2 \ . \tag{B.4}$$

The moment at the middle of the elbow is

$$M_e = F_x(L_2 - 0\ 2929R) + 0.2929\ F_yR + M_2 \ . \tag{B.5}$$

NUREG/CR-3599
ORNL/Sub/82-22252/2
Dist. Category RM

Internal Distribution

1. C. R. Brinkman
2. J. A. Clinard
3. C. W. Collins
4. J. M. Corum
5. D. M. Eissenberg
6. D. S. Griffith
7. R. C. Gwaltney
8. W. R. Hendrich
9. R. L. Huddleston
10. Y. L. Lin
11. W. L. Greenstreet
12. A. P. Malinauskas
13. S. S. Manson (Consultant)
14. J. E. Moore
15. J. E. Pugh
16. H. E. Trammell
17. G. D. Whitman
18-22. G. T. Yahr
23-26. Structural Design Criteria, 9204-1, MS 11
27. ORNL Patent Office
28. Central Research Library
29. Document Reference Section
30-31. Laboratory Records Department
32. Laboratory Records (RC)

External Distribution

33. Office of Assistant Manager for Energy Research and Development, Department of Energy, ORO, Oak Ridge, TN 37830
34-35. Technical Information Center, DOE, Oak Ridge, TN 37830
36-335. Given distribution as shown under category RM (NTIS-10)
336-467. Special ASME Code Distribution (by NRC)

NRC FORM 335 (11-81)

U.S. NUCLEAR REGULATORY COMMISSION

BIBLIOGRAPHIC DATA SHEET

1. REPORT NUMBER (Assigned by DDC)
NUREG/CR-3599
ORNL/Sub/82-22252/2

4. TITLE AND SUBTITLE (Add Volume No., if appropriate)
Sources of Uncertainty in the Calculations of Loads on Supports of Piping Systems

2. (Leave blank)

3. RECIPIENT'S ACCESSION NO.

7. AUTHOR(S)
E. C. Rodabaugh

5. DATE REPORT COMPLETED
MONTH: May YEAR: 1984

9. PERFORMING ORGANIZATION NAME AND MAILING ADDRESS (Include Zip Code)
E. C. Rodabaugh Associates, Inc.
4625 Cemetery Road
Hilliard, Ohio 43026

DATE REPORT ISSUED
MONTH: June YEAR: 1984

6. (Leave blank)

8. (Leave blank)

12. SPONSORING ORGANIZATION NAME AND MAILING ADDRESS (Include Zip Code)
Division of Engineering Technology
Office of Nuclear Regulatory Research
U.S. Nuclear Regulatory Commission
Washington, DC 20555

10. PROJECT/TASK/WORK UNIT NO.

11. FIN NO.
B0474

13. TYPE OF REPORT
Topical

PERIOD COVERED (Inclusive dates)

15. SUPPLEMENTARY NOTES

14. (Leave blank)

16. ABSTRACT (200 words or less)

Loads on piping systems are obtained from an analysis of the piping system. The piping system analysis involves uncertainties from various sources. These sources of uncertainties are discussed and ranges of uncertainties are illustrated by simple examples. The sources of uncertainties are summarized and assigned a judgmental ranking of the typical relative significance of the uncertainty.

17. KEY WORDS AND DOCUMENT ANALYSIS

17a. DESCRIPTORS

17b. IDENTIFIERS/OPEN-ENDED TERMS

18. AVAILABILITY STATEMENT
Unlimited

19. SECURITY CLASS (This report)
Unclassified

21. NO. OF PAGES

20. SECURITY CLASS (This page)
Unclassified

22. PRICE
$

120555078877 1 1AN1RM
US NRC
ADM-DIV OF TIDC
POLICY & PUB MGT BR-PDR NUREG
W-501
WASHINGTON DC 20555